1998-09

An analysis of a broadband multicarrier CDMA cellular communications system

Pace, Howard

http://hdl.handle.net/10945/32765

NAVAL POSTGRADUATE SCHOOL
Monterey, California

THESIS

AN ANALYSIS OF A BROADBAND MULTICARRIER CDMA CELLULAR COMMUNICATIONS SYSTEM

by

Howard Pace, Jr.,

September 1998

Thesis Advisor:	Tri Ha
Co-Advisor:	R. Clark Robertson

Approved for public release; distribution is unlimited.

19981015 108

REPORT DOCUMENTATION PAGE

Public reporting burden for this collection of information is estimated to average 1 hour per response, including the time for reviewing instruction, searching existing data sources, gathering and maintaining the data needed, and completing and reviewing the collection of information. Send comments regarding this burden estimate or any other aspect of this collection of information, including suggestions for reducing this burden, to Washington Headquarters Services, Directorate for Information Operations and Reports, 1215 Jefferson Davis Highway, Suite 1204, Arlington, VA 22202-4302, and to the Office of Management and Budget, Paperwork Reduction Project (0704-0188) Washington DC 20503.

1. AGENCY USE ONLY *(Leave blank)*	2. REPORT DATE September 1998	3. REPORT TYPE AND DATES COVERED Master's Thesis

4. TITLE AND SUBTITLE AN ANALYSIS OF A BROADBAND MULTICARRIER CDMA CELLULAR COMMUNICATIONS SYSTEM	5. FUNDING NUMBERS
6. AUTHOR(S) Howard Pace, Jr.,	

7. PERFORMING ORGANIZATION NAME(S) AND ADDRESS(ES) Naval Postgraduate School Monterey, CA 93943-5000	8. PERFORMING ORGANIZATION REPORT NUMBER

9. SPONSORING/MONITORING AGENCY NAME(S) AND ADDRESS(ES)	10. SPONSORING/MONITORING AGENCY REPORT NUMBER

11. SUPPLEMENTARY NOTES The views expressed in this thesis are those of the author and do not reflect the official policy or position of the Department of Defense or the U.S. Government.

12a. DISTRIBUTION/AVAILABILITY STATEMENT Approved for public release; distribution is unlimited.	12b. DISTRIBUTION CODE

13. ABSTRACT *(maximum 200 words)*

The integration of land, sea, and air forces within the littoral environment will require fading resistant, high data rate, non-exploitable communications. The large volumes of video and data information, i.e. Internet access, video teleconferencing and data transfer, required to support the war fighter within a Joint Task Force demands technologies that reduce the interference imposed by poor terrestrial and atmospheric conditions. In order to minimize the effect of frequency-selective fading that occurs in these conditions and to provide high data rate communications, this thesis presents the analysis of a broadband cellular system featuring a multicarrier, code division multiple access (CDMA) method. The system designed complies with Federal Communication Commission broadband cellular standards and uses CDMA to reduce the probabilities of detection and interception as well as providing for multiple access, which in conjunction with the multicarrier approach enables on demand access to high data rate communications.

14. SUBJECT TERMS Littoral Communications, Analysis, Cellular, CDMA, Broadband, Multicarrier	15. NUMBER OF PAGES 118
	16. PRICE CODE

17. SECURITY CLASSIFICATION OF REPORT Unclassified	18. SECURITY CLASSIFICATION OF THIS PAGE Unclassified	19. SECURITY CLASSIFICATION OF ABSTRACT Unclassified	20. LIMITATION OF ABSTRACT UL

i

AN ANALYSIS OF A BROADBAND MULTICARRIER CDMA CELLULAR COMMUNICATIONS SYSTEM

Howard Pace, Jr.,
Lieutenant, United States Navy
Bachelors of Science Mechanical Engineering, University of Washington, 1990

Submitted in partial fulfillment
of the requirements for the degree of

**MASTER OF SCIENCE
IN
ELECTRICAL ENGINEERING**

from the

NAVAL POSTGRADUATE SCHOOL
September 1998

Author: _____
Howard Pace, Jr.,

Approved by: _____
Tri Ha, Thesis Advisor

_____
R. Clark Robertson, Co-Advisor

_____
Jeffrey B. Knorr, Chairman
Department of Electrical and Computer Engineering

iii

ABSTRACT

The integration of land, sea, and air forces within the littoral environment will require fading resistant, high data rate, non-exploitable communications. The large volumes of video and data information, i.e. Internet access, video teleconferencing and data transfer, required to support the war fighter within a Joint Task Force demands technologies that reduce the interference imposed by poor terrestrial and atmospheric conditions. In order to minimize the effect of frequency-selective fading that occurs in these conditions and to provide high data rate communications, this thesis presents the analysis of a broadband cellular system featuring a multicarrier, code division multiple access (CDMA) method. The system designed complies with Federal Communication Commission broadband cellular standards and uses CDMA to reduce the probabilities of detection and interception as well as providing for multiple access, which in conjunction with the multicarrier approach enables on demand access to high data rate communications.

TABLE OF CONTENTS

LIST OF FIGURES

LIST OF TABLES

I. HIGH DATA RATE CELLULAR COMMUNICATIONS

A. TODAY'S CELLULAR SERVICE

Cellular communication services have experienced explosive growth in the last decade. Originally used exclusively for voice communications, cellular systems are now used to provide low data rate information, comparable to information transfer rates provided by paging services. These applications are limited to data rates around 9600 bits per second. The global work force of today demands mobility and unlimited timely information access, and these low data rate narrow band systems prove to be unacceptable.

New and exciting applications will be achievable if wireless data rates are improved. For example, higher data rates can be used in the development of more advanced wireless phone systems. These systems will provide a variety of mobile services such as large data file transfer, video teleconferencing (VTC), and full Internet connectivity. Another example is in the medical emergency response field. Imagine the improvement in medical care if the emergency room staff were able to receive a patient's complete medical status from the ambulance in route to the hospital. X-ray exams, live video for triage analysis, and vital sign monitoring results could all be sent real time. In recognition of these new consumer requirements, the Federal Communications Commission (FCC) has established new standards for these cellular systems, appropriately dubbed broadband Personal Communications Systems (PCS) [Ref. 1].

B.   BROADBAND PCS

Broadband PCS are loosely defined by the FCC as "radio communications that encompass mobile and ancillary fixed communication services that provide services to individuals and businesses and can be integrated with a variety of competing networks." [Ref. 1]. Broadband PCS are allocated to the band of the electromagnetic spectrum from 1850 to 1990 MHz, and the bandwidth allocated for broadband PCS totals 120 MHz. The extraordinary growth potential in the broadband PCS market has resulted in the most profitable spectrum auction in FCC history. The auction of the first portion of broadband PCS during fiscal years 1994 and 1995 generated 7.7 Billion dollars for the United States Treasury [Ref. 1]. It is estimated that there are currently twenty million wireless telephone subscribers in the United States today. Some analysts predict that in ten years there will be one hundred million subscribers. The creation of this new broadband PCS market is estimated to generate tens of billions of dollars of future investments [Ref. 1].

C.   BROADBAND PCS SPECTRUM

As shown in Table 1.1, the FCC has divided the 120 MHz bandwidth of the broadband PCS spectrum into six frequency blocks (A thru F). These blocks are categorized, based on anticipated revenues, as either a Major Trading Area (MTA) or a Basic Trading Area (BTA). There are 51 MTAs and 493 BTAs throughout the United States and its possessions [Ref. 1].

The broadband PCS spectrum breakdown is:

Block Name	Block Size	Geographic Breakdown	Results
Block A	30 MHz	MTA	Licensed Jun 96
Block B	30 MHz	MTA	Licensed Jun 95
Block C	30 MHz	BTA	Licensed 482 of 493 BTAs, Jan 97
Block D	10 MHz	BTA	Licensed for all 493 BTAs, Nov 97
Block E	10 MHz	BTA	Licensed for all 488 BTAs, Sep 97
Block F	10 MHz	BTA	Licensed 483 of 491 BTAs, Nov 97

Table 1.1. FCC assigned broadband PCS spectrum.

Each service area will have multiple service providers. Each service region has a total of 120 MHz bandwidth available. Twenty MHz will be reserved for unlicensed applications that will include both data and voice services. The remaining 100 MHz is divided between MTAs, BTAs, or a combination of both. In order to support full duplex, simultaneous radio transmission and reception between a subscriber and a base station, half of the bandwidth is assigned to the forward channel, from base to mobile, and the other half is assigned to the reverse channel, from mobile to base. As an example, a MTA will have 30 MHz of assigned bandwidth, 15 MHz assigned to the forward channel and 15 MHz assigned the reverse channel. Other FCC requirements include [Ref. 1]:

Field Strength	47 dBμ volt/meter (At the border of each cell.)
Maximum base antenna height	300 meters
Maximum power each mobile	2 Watts peak EIRP
Maximum power each base station	1640 Watts peak EIRP

In an attempt to keep government regulation to a minimum, the FCC has provided very few standard requirements for broadband PCS [Ref. 1]. When one compares regulatory requirements for IS 95, the standard for narrow band Code Division Multiple Access (CDMA) cellular communications, to the broadband PCS standard, it is immediately clear how much regulation has been avoided. However, as with all communication systems, the unavoidable issue of limited bandwidth, and the corresponding bit rate, must be addressed. Given the maximum bandwidth available for either the forward or reverse channel is 15 MHz, what are the practical limits to a broadband PCS design?

D. MOTIVATION FOR MULTICARRIER SYSTEMS

1. Fading

To answer the bandwidth issue, we must first understand the basic mechanisms that affect the communications link. As the communications signal propagates from the transmitter to the receiver, energy is lost due to scattering, reflection, and diffraction. Mobile channels are typically modeled as fading channels, where the fading is characterized by a combination of large and small scale fading. For subscriber motion over distances large compared to a wavelength, fluctuations in receiver signal strength are characterized as large scale fading. Large scale fading represents the channel loss introduced by the mobile channel.

When the received signal rapidly changes in amplitude and phase for subscriber motion over very short distances compared to a wavelength, then small scale fading, or simply fading, has occurred. When transmitting in unguided mediums, like the atmosphere, the signal can arrive at the receiver via multiple paths. These multiple paths can be due to obstructions, which prevent line-of-sight communications, ground reflections, or scattering within the channel. The receiver sums the multipath contributions; but since the multipath components vary widely in phase, the signal at the

receiver can also fluctuate widely. Subsequently, the sum of the multipath components can be either constructive or destructive.

2.   Small Scale Fading

Multipath in the channel creates small scale fading effects. The three most important effects are [Ref. 2]:

a.   Rapid changes in received signal strength over distances short compared to a wavelength.

b.   Random frequency modulation due to varying Doppler shifts on different multipath signals.

c.   Time dispersion caused by multipath propagation delays.

Currently, no model exists that will predict how each channel will behave. Furthermore, changes in the weather or the installation or removal of objects like buildings or trees will change the channel. Impulse response tests of the channel are conducted to form a power delay profile, which is used to determine channel characteristics. By using a transmitter to send a pulse that approximates a delta function through the channel, the channel response can be measured and evaluated. Measurements are generally made at intervals corresponding to a quarter of the transmitting wavelength. Taking the spatial average of the responses, we obtain an ensemble of power delay profiles for the channel.

3.   Fading Effects Due to Multipath Time Delay Spread

The root mean square (rms) delay spread is the square root of the second central moment of the power delay profile. The mean excess delay is the first moment of the power delay profile or as the name suggests, the mean delay value. These values provide

5

the method to gauge how rapidly the channel changes in the time domain [Ref. 3]. The power delay profile and the magnitude frequency response are related by the Fourier transform.

The delay spread in the time domain is analogous to the coherence bandwidth in the frequency domain. The channel coherence bandwidth and is used to characterize the channel, and is defined as the range of frequencies over which the channel's response is relatively flat [Ref. 3]. This means the amplitude correlation between two signals within the channel coherence bandwidth is very high. The degree of correlation required is essentially a performance driven requirement that can be adjusted depending on the application.

If the transmitted signal bandwidth B_s is much greater than the channel coherence bandwidth B_c, $B_s \gg B_c$, then the received signal will be distorted by inter-symbol interference (ISI) [Ref. 3]. This is called frequency selective fading. If the transmitted signal bandwidth is much less than the channel coherence bandwidth, $B_s \ll B_c$, then the signal's spectral components will be passed with approximately equal gain and linear phase. This is called flat fading [Ref. 3]. The Rayleigh distribution is used to model the statistical time varying nature of the received signal for the mobile wireless channel with flat fading.

An exact relationship between channel coherence bandwidth B_c and the rms delay spread σ_τ does not exist. The channel coherence bandwidth is related to the rms delay spread empirically by

$$B_c \approx \frac{1}{X\sigma_\tau} \qquad (1.1)$$

where X is a parameter that is determined by how conservative of an estimate is desired.

If B_c is defined to be the bandwidth over which the frequency correlation is above ½,

then X = 5 [Ref. 3]:

$$B_c \approx \frac{1}{5\sigma_\tau} \qquad (1.2)$$

This is considered a very conservative estimation of B_c. A less conservative estimate is

X = 1 [Ref. 2]:

$$B_c \approx \frac{1}{\sigma_\tau} \qquad (1.3)$$

For a narrowband mobile system, [Ref. 3] gives $B_c = 800kHz$, while [Ref. 2] gives

$B_c = 5MHz$. Using these values in Equation 1.2 and Equation 1.3, we get $\sigma_\tau = 0.14\mu s$.

Hence, for this thesis we use:

$$B_c = \frac{1}{2.9\sigma_\tau} = 2.5MHz \qquad (1.4)$$

as a reasonable compromise between Equations 1.2 and 1.3.

4.   Fading Effects Due to Doppler Shift

The relative motion between the transmitter and the receiver results in random

frequency modulation due to different Doppler shifts on each of the multipath

components. Additionally, any motion of the objects obstructing the channel will also

cause a corresponding time varying Doppler shift.

The relative velocity of the transmitter and receiver, along with the velocity of

objects in the channel and how rapidly the baseband signal changes as compared to the

rate of change of the channel response, determines the degree to which Doppler shift will affect the signal's reception. This Doppler shifted fading is classified into two categories, fast fading and slow fading channels. In the frequency domain, fast fading occurs when the Doppler spread B_d is greater than the baseband signal's bandwidth B_s. This is related to the channel coherence time by [Ref. 3].

$$(\Delta t)_c \cong \frac{1}{B_d} \tag{1.5}$$

Fast fading causes signal distortion. A slow fading channel occurs when $B_s \gg B_d$. This implies a slow fading channel is of constant amplitude and linear phase over several reciprocal bandwidth intervals.

5. Bandwidth Limitations Caused by Fading Effects

To determine the maximum theoretical bit rate a system is capable of achieving, the designer can use the Shannon channel capacity, valid for additive white Gaussian noise (AWGN), [Ref. 3]:

$$C = B\log_2(1 + SNR) \tag{1.6}$$

where B = system bandwidth, 15 MHz for broadband PCS, SNR = signal-to-noise ratio, ranging from 12 to 24 dB for broadband PCS, and C = channel capacity.

Given these parameters, for broadband PCS the channel capacity ranges from 51.9 to $119.7 Mb/s$. But Shannon's capacity equation does not consider constraints such as fading. To avoid ISI and distortion effects of fast frequency selective fading, the system's baseband bandwidth must meet the requirements for both flat and slow fading. The system baseband bandwidth must be greater then the Doppler bandwidth and remain lower then the channel coherence bandwidth.

The Doppler bandwidth for a mobile moving in the x direction with constant velocity is [Ref. 4].

$$B_d = f_m \cos \alpha \qquad (1.7)$$

where f_m is the Doppler frequency related to the phase change resulting from changes in path length between the transmitter and receiver and $f_m = \dfrac{V}{\lambda}$. The mobile's velocity is represented by V and the carrier frequency's wavelength is λ. The parameter α is the spatial angle between the direction of travel and the path between the receiver and the transmitter. If the mobile is traveling at 65 miles per hour and the carrier frequency is 1920 MHz, then the corresponding B_d is 186.0 Hz. Given a PCS baseband bandwidth of 15 MHz, $B_s >> B_d$. Therefore, the PCS channel can generally be modeled as slowly fading. For broadband PCS, the challenge is to design a system that is not frequency selective.

For fading to remain flat we determined from Equation 1.4 that

$$T_c \geq 2.9 \sigma_\tau \qquad (1.8)$$

where T_c is the duration of each individual pulse transmitted over the channel.

Using Equation 1.8 we get

$$T_c \geq 0.4 \, \mu s \qquad (1.9)$$

for broadband PCS.

Given T_c, for binary modulation and CDMA, the channel bit duration is obtained from

$$T_b = N T_c \qquad (1.10)$$

where N is number of chips per bit contained in the PN spreading sequence.

The selection of N must be carefully considered. The larger the value of N, the more bandwidth the system will require for a given bit rate. However, large N will also improve the system's ability to reduce co-user interference, a very important feature for CDMA systems. This tradeoff is best evaluated during performance analysis of the system where the designer can clearly review performance; i.e., probability of bit error (P_b) vs. bandwidth and bit rate.

If we assume binary-phase shift keying (BPSK) or differential-phase shift keying (DPSK) modulation and N = 15, then from Equation 1.10

$$T_b \geq 6.0\,\mu s \tag{1.11}$$

for broadband PCS. Hence, the maximum achievable channel bit rate R_b that will allow flat, slow fading is found by taking the reciprocal of T_b:

$$R_b \leq 170\,\frac{kbits}{s} \tag{1.12}$$

The use of forward error correction coding (FEC) can greatly improve performance. FEC codes provide redundant bits, which are transmitted with the data bits. In the event of an error, these additional bits, or parity bits, are used to identify the bit or bits in error and, depending on the type of code and the number of errors, correct the errors. For example, if a rate ½ convolutional code is used, for each data bit transmitted a parity bit is also transmitted. In general, k information bits and n-k parity bits are transmitted, and the code rate (r_c) is $\left(\dfrac{k}{n}\right)$. The use of FECs comes with a cost.

Specifically, the additional overhead bits reduce the information bit rate by a factor of r_c. The resulting information bit rate with coding is related to the channel bit rate by

10

$$R_s = r_c R_b \tag{1.13}$$

which for broadband PCS yields a maximum of

$$R_s \leq 85 \frac{kbits}{s} \tag{1.14}$$

when 11.8 dB of spreading is used.

6. The Use of Multicarrier Systems to Improve Bit Rate

The maximum information bit rate for broadband PCS obtained in the last section is more than double the current narrowband CDMA cellular bit rate of 9600 bits/second [Ref. 3]. Although this is an improvement, it is clearly not what is necessary to deliver the large volumes of data required for wireless Internet operations. How then can larger data rates be produced if the limiting factor is the channel coherence bandwidth, which, once exceeded, will cause prohibitive distortion? One possibility is to use a multi-carrier CDMA system as illustrated in Figure 1.1.

In a multicarrier CDMA system, the data stream is broken up into as many as M bit streams that are individually transmitted on up to M different frequencies $(f_1, f_2, ... f_M)$, where the subscript $i = 1, 2, 3, ..., M$ uniquely identifies the carrier frequency. Hence, multicarrier CDMA can be thought of as a hybrid of FDMA and CDMA.

11

DS/DPSK
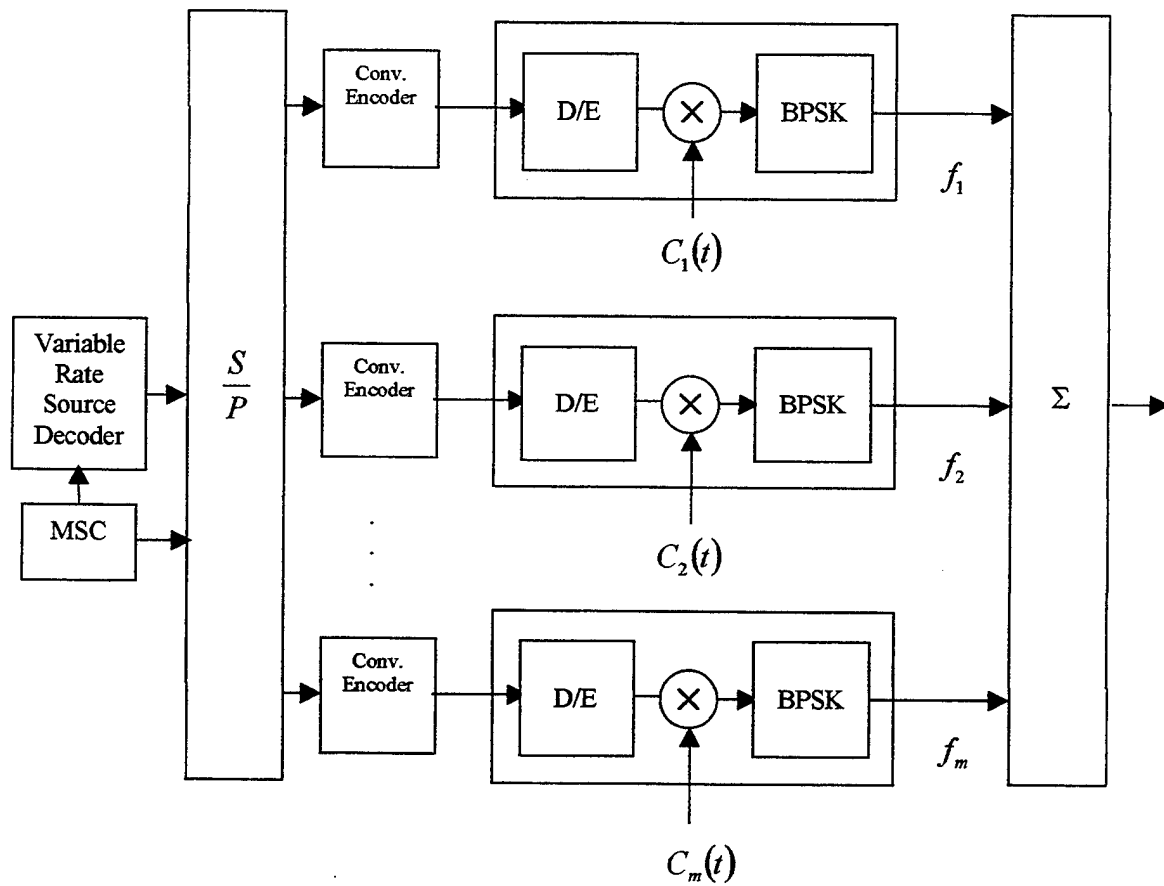
Figure 1.1. An example of a multicarrier transmitter circuit.

A multicarrier system transmitter is shown in Figure 1.1. Each branch in Figure 1.1 represents one of the M carriers. Depending on traffic intensity, the mobile switching center (MSC) determines the data rate that each mobile will be assigned, and transmits that information via the forward link. The variable rate source encoder changes the information rate from the source to comply with the MSC ordered data rate, while the serial-to-parallel multiplexer assigns the appropriate number of carrier frequencies. The data stream undergoes serial-to-parallel conversion appropriate to the number of carriers assigned by the MSC. The data stream for each carrier is sent through a convolutional encoder, then differentially encoded, spread, and modulated. Finally the output of each branch is summed and transmitted out the mobile antenna.

For BPSK or DPSK, a single carrier system provides a data rate equal to R_S. For a multicarrier system having the same data rate, each of the M multicarrier system frequencies will provide a data rate equal to

$$R_{s_i} = \frac{R_S}{M} \tag{1.15}$$

Therefore, the bandwidth of each multicarrier frequency B_{s_i} is 1/M times smaller than that of the single carrier system. This means the multicarrier system is more likely to remain frequency non-selective than an equivalent single carrier system. To ensure flat fading for each carrier, the signal bandwidth for each carrier is designed to be less than the channel coherence bandwidth, $B_{s_i} < B_c$.

The maximum number of carriers that are possible are obtained by taking the ratio of the channel bandwidth and the bandwidth of the signal on each carrier:

$$M = \frac{B}{(1+\alpha)\left(\dfrac{R_{s_i}}{r_c}\right)N} \qquad (1.16)$$

where B is the overall system bandwidth, α is a weighting coefficient, ½ for raised cosine filters, N is the number of chips per bit, and r_c is the code rate. For flat fading, we require $B_c \geq (1+\alpha)\left(\dfrac{R_{s_i}}{r_c}\right)N$. Using B = 15 MHz, α = ½, N =15, and r_c = ½, we obtain the maximum number of six carriers. Six carriers and four users using all of the available 15 MHz of assignment bandwidth can deliver 1.36 $Mbits/s$ for the reverse channel, and 5.1 $Mbits/s$ for the forward channel, a significant increase in data rate over either narrowband cellular or broadband PCS without multicarrier CDMA.

II. ANALYSIS OF FORWARD LINK PERFORMANCE USING MULTI-CARRIER DS/BPSK, WALSH-HADAMARD SPREADING, CONVOLUTIONAL CODING, AND SOFT DECISION DECODING

A. MULTIPLE ACCESS AND INTERFERENCE

The principle advantage to a multi-carrier system is the ability to deliver variable date rates on demand and minimize fading effects. As the customer requires higher data rates, the MSC will decide how many of the available carriers will be assigned to each user. This decision is based on priority and traffic intensity. Unlike other multiple access techniques, a CDMA system does not separate the users with frequency or time assignments. Instead, these users are separated through the use of orthogonal, or nearly orthogonal, spreading codes. These codes are exclusively OR with the data sequence prior to heterodyning and transmitting.

In the case of the forward link, the transmitter is the base station and the receiver is the user, or mobile. The receiver bandwidth is equal to the FCC assignment of 15 MHz [Ref. 1]. The forward channel uses the Walsh-Hadamard functions for spreading. The orthogonal property of the Walsh-Hadamard spreading codes allows the signal from the base station to the desired user to be recovered from among the other unwanted base station signals. The correlation between the receiver's despreading code and the unwanted user's spreading code is small. Therefore, as the received signal is multiplied by the despreading code, the unwanted signals from the base station to other users are not despread.

In general, the cost of a CDMA system comes in two forms of user generated interference. The first occurs within the cell in question, hereby referred to as the reference cell, and is the result of the additive effect of the unwanted signals described in the previous paragraph. This type of noise is called intra-cell, multi-user interference, and is ideally zero when Walsh-Hadamard spreading codes are used.

The second type of interference is referred to as co-channel interference. Co-channel interference originates from the base stations of adjacent cells. If a single cell CDMA system is used, then the entire available bandwidth of the system is re-used in each cell. Each mobile receives all signals within that given bandwidth. These signals may, in addition to the unwanted base station to user signals contained within the reference cell, include co-channel interference from the adjacent cells. Each base station has a unique PN spreading sequence and each user within the cell has a unique Walsh-Hadamard spreading code. Together these spreading sequences prevent interference from adjacent cells with the same spreading sequence. It is important to note that the forward link interference in the intra-cell, multiuser and co-channel cases does not originate from the mobiles, but from the base stations. Figure 2.1 shows an example of intra-cell, multiuser and co-channel interference.

Base station	⋀
User of interest within the reference cell	☺
Co-channel interference	⊘
Intra-cell multi-user interference	⊚
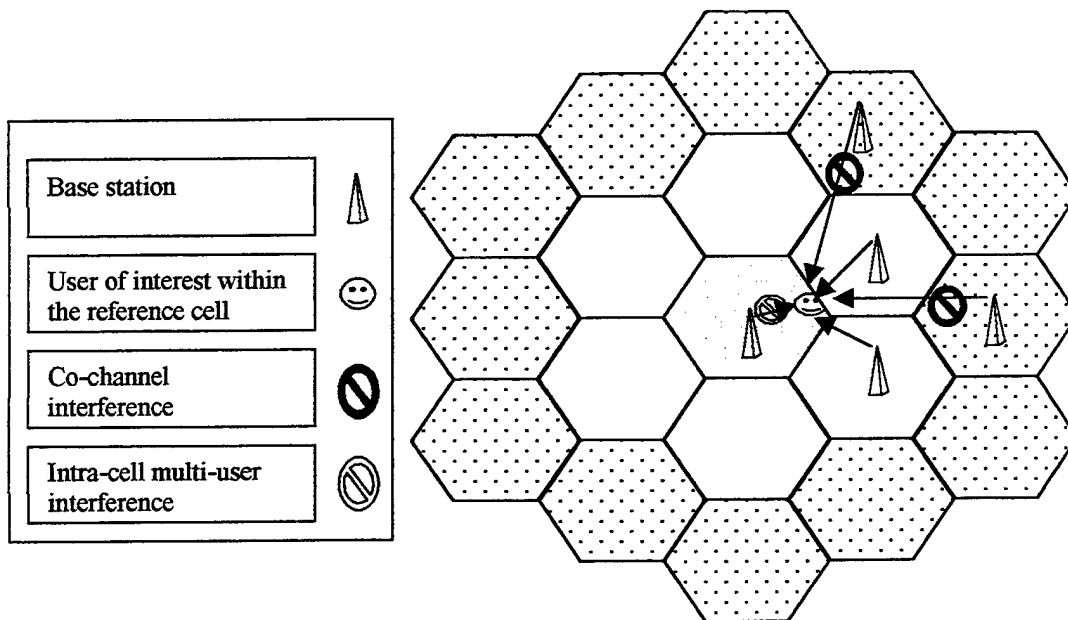
Figure 2.1. Forward channel interference.

Given poor environmental conditions and spatial separation between cells, the co-channel interference may be so severe that several tiers of cells surrounding the reference cell may contribute to the overall co-channel interference problem. As shown in Figure 2.2, those cells immediately around the reference cell are known as the first tier, while the second ring of cells that surround the reference cell and the first tier cells are known as the second tier. Each may contribute to the co-channel interference problem.

Reference cell, White
1st Tier cells, Gray
2nd Tier cells, Pattern
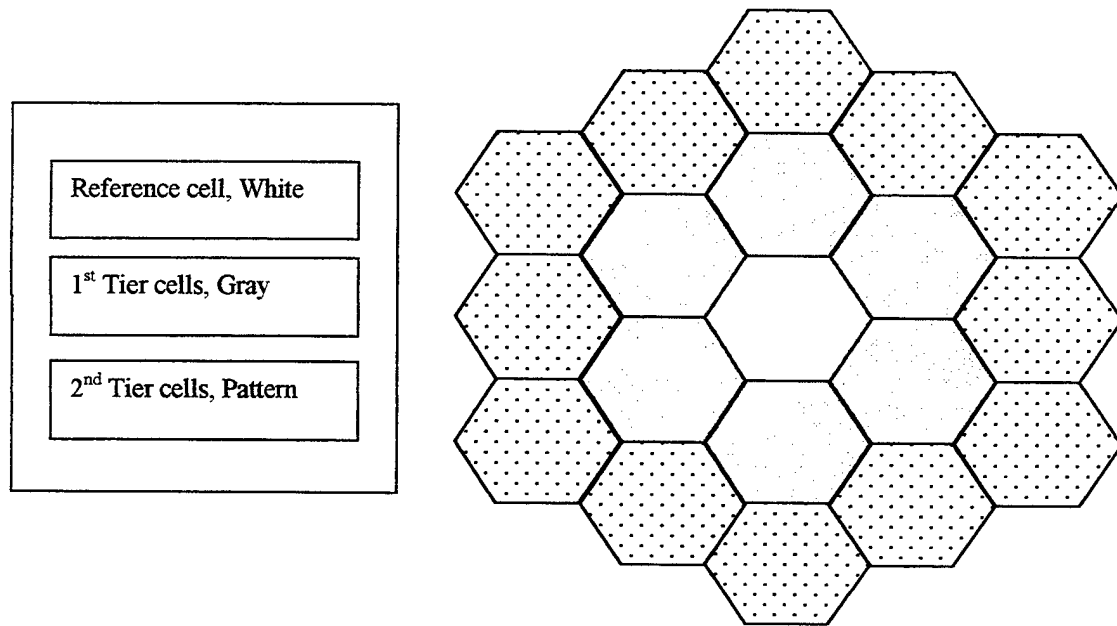
Figure 2.2. Tier cell arrangement.

The effects of co-channel interference can be reduced. Increasing the cell radius, sectoring, employing micro-zone techniques, or controlling the number of users per cell will decrease co-channel interference. Increased signal power will not reduce co-channel interference. On the contrary, increased base station power will add to the co-channel interference problem. For the purposes of this thesis we will assume that the cell design effectively reduces the second tier co-channel interference to the point it is negligible compared to the first tier co-channel interference. Therefore, the analysis of forward channel will neglect second tier co-channel interference.

B. MODULATION

Selection of the modulation technique is based on performance and system requirements. Additionally, the maximum data rate required is anticipated on the forward link. For example, when using the Internet, a user's inputs occur via the reverse link. Typically these inputs represent a request for frames of data to be transferred to the user via the forward link. The bulk of the high data rate transfer will occur on the forward link.

The user is assumed to be using a notebook size device. Physical size limits the complexity of the transmitter and receiver. Noncoherent receivers do not require pilot tones, are easy to build, and relatively inexpensive but require greater received signal-to-noise ratio as compared to a coherent receiver. The spectral efficiency of M-ary phase shift keying (MPSK) is superior to M-ary frequency-shift keying (MFSK). For example, the null-to-null bandwidth of binary PSK (BPSK) is twice the bit rate $(2R_b)$. The corresponding BFSK bandwidth as given by Carson's rule is

$$BW_{BFSK} = 2R_b + 2\Delta f. \qquad (2.1)$$

$$\Delta f = \text{frequency deviation} \qquad (2.2)$$

BPSK is more bandwidth efficient then BFSK by a factor of $2\Delta f$.

To prevent distortion, MPSK must use linear power amplifiers, where as MFSK can use non-linear amplifiers. MFSK transmitters may provide higher output signals than MPSK transmitters. MFSK can also place more power into the main lobe of the communications signal and less into the side lobes and can be received noncoherently. Only special variations of MPSK such as differential MPSK (MDPSK) signals can be received noncoherently.

The forward link employs a pilot tone to provide many essential forward link features. A pilot tone delivers a phase reference for coherent demodulation and timing information that allows spreading code synchronization. For a given probability of bit error, a coherent receiver requires less signal-to-noise ratio than a noncoherent receiver. Another benefit of the pilot channel is that it provides the means for the mobile to compare base station signal strengths for hand-off purposes and allows the mobile to acquire timing for the forward CDMA channel.

One additional consideration must now be discussed, the issue of power control. When several users occupy the same cell, as shown in Figure 2.3, the user closest to the base station is assumed to have lower path loss, hence a higher signal-to-noise ratio. This reverse link condition may permit the closer user to dominate the receiver and prevent the proper recovery of users further away from the base station. This problem is known as the "near far-effect". Therefore, an essential requirement of the forward link will be to provide a method to equalize the power received at the base station from all transmitting users.
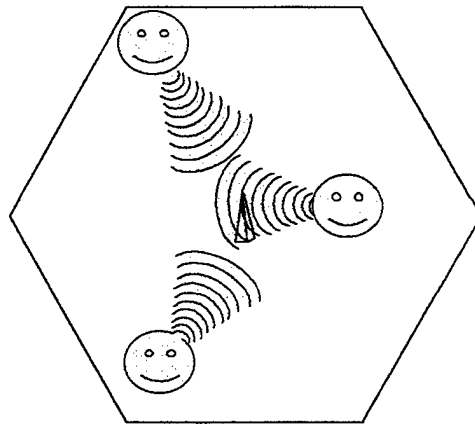
Figure 2.3. The "near-far effect".

The mobility of the user and the rapid power changes due to fading requires fast power equalization. To meet this demand, a combination of fast, open and closed looped power controls must be used [Ref. 3]. These power controls must adjust the reverse link transmitter power of each mobile within the cell, such that the base station receives each user with the same power level. To provide the means to combat the near-far effect, the multi-carrier system will also require power control information within the forward link traffic.

1. **Comparison of Modulation Techniques in a Frequency-nonselective, Slowly Fading Channel**

As the frequency non-selective channel slowly fades, the base station to user signal is subjected to multiplicative distortion. The nature of the slowly fading channel requires the multiplicative process to be constant for at least one signal interval. It is assumed that the channel fading is sufficiently slow to allow the phase shift to be estimated from the pilot tone without error.

To examine the performance of different coherently received binary modulation techniques, one may evaluate the decision variables and then determine the probability of bit error. Given a fixed attenuation, α, in a non-fading channel, the probability of bit error for a BPSK system is

$$P_b = Q\left(\sqrt{\frac{2E_b(\alpha^2)}{N_o}}\right) \qquad (2.3)$$

However, in a fading channel the attenuation factor is no longer fixed, and the BPSK probability of bit error is now conditioned on the attenuation factor α. The conditional BPSK probability of bit error is

21

$$P_b(\gamma_b) = Q(\sqrt{2\gamma_b}) \tag{2.4}$$

where the received signal-to-noise ratio γ_b is given by

$$\gamma_b = \left(\frac{\alpha^2 E_b(\alpha^2)}{N_o} \right) \tag{2.5}$$

To find the unconditional BPSK probability of bit error, P_b, the product of the conditional probability of bit error, $P_b(\gamma_b)$, and the probability density function (pdf), $p(\gamma_b)$, of the random variable γ_b must be integrated over the range of γ_b. The attenuation factor α, is modeled as Rayleigh distributed; therefore, α^2 is a chi-squared random variable. This implies that γ_b must also be chi-square-distributed. The resulting pdf is [Ref. 2]

$$p(\gamma_b) = \left(\frac{1}{\overline{\gamma_b}} \right) e^{-\left(\frac{\gamma_b}{\overline{\gamma_b}} \right)} \qquad \gamma_b \geq 0 \tag{2.6}$$

where $\overline{\gamma}_b$ is the average signal to noise ratio and is given by

$$\overline{\gamma}_b = \frac{\overline{E_b}}{N_o} \tag{2.7}$$

where $\overline{E_b}$ is the expected value of $E_b(\alpha^2)$. Carrying out the proceeding, we obtain

$$P_b = \int_0^\infty P_b(\gamma_b) p(\gamma_b) d\gamma_b \tag{2.8}$$

which can be evaluated to obtain the probability of bit error for BPSK as [Ref. 2]

$$P_b = \frac{1}{2} \left(1 - \sqrt{\frac{\overline{\gamma_b}}{1 + \overline{\gamma_b}}} \right) \tag{2.9}$$

The probability of bit error P_b for QPSK is the same as BPSK and provides twice the bit rate, all other things being equal, at the expense of some additional complexity. DPSK requires slightly higher signal-to-noise ratio (SNR) than BPSK. Although DPSK can be received noncoherently, the use of a pilot tone on the forward link allows for coherent reception.

Now the question remains, can a BPSK system satisfy the performance requirement for the forward link? Satisfactory performance will be defined as a probability of bit error smaller than 10^{-5} for a given SNR γ_b of twelve dB. For $\gamma_b = 12$ dB, the probability of bit error of coherent BPSK over a Rayleigh fading channel is 10^{-2} [Ref. 2]. This clearly does not reach the performance goal of 10^{-5}. Additionally, the analysis of the probability of bit error for BPSK excluded all forms of interference. As described earlier, the system will be subjected to co-channel interference as well as additive white Gaussian noise (AWGN). How can the performance of the coherent BPSK system be enhanced to meet the required probability of bit error?

C.   FORWARD ERROR CORRECTION CODING

Given the harsh environment imposed by a fading channel, a designer must consider every means possible to improve the system's performance. One such method is forward error correction coding (FEC). Essentially, FEC introduces an additional number of data bits, which are appended to the original information for the purpose of detecting and/or correcting errors. The number and pattern in which these redundant data bits are appended to the information enhances the correct recovery of the information bit stream.

For every k information data bits, a corresponding number of n coded bits are transmitted. The total number of n coded bits is equal to the number of information bits plus those redundant code bits added to identify and/or correct errors. The code rate of a FEC is

$$r_c = \frac{k}{n} \qquad (2.10)$$

The purpose of adding these additional bits is to improve the system's performance, i.e., probability of bit error, without increasing SNR. Coding gain is defined as the difference in the signal-to-noise ratios required by a FEC coded system and the same un-coded system to achieve a specific probability of bit error

$$G_{dB} = \left(\frac{E_b}{N_o}\right)_{uncoded} - \left(\frac{E_b}{N_o}\right)_{coded} \qquad (2.11).$$

Coding gain can be positive or negative and can be as high as 8 dB [Ref. 2]. The amount of coding gain depends upon the type of FEC code, modulation technique, and type of errors.

There are primarily two types of errors: random errors and burst errors. Random errors are typically caused by AWGN. Burst errors occur in clusters, within a relatively short period of time, and are caused by large fluctuations in signal-to-noise ratio. A primary example of a burst error source is a fading channel.

One method to combat burst errors is through the use of interleaving. Burst errors occur in consecutive sequences. Interleaving separates the burst errors in an attempt to break up error bursts such that the FEC may correct these errors. Interleaving divides up the coded information bits in a pre-arranged order. If errors occur, the de-interleaving will disperse these errors among the remainder of the information bits prior to the

decoder. The larger the interleaver, the longer the burst error distance that can be tolerated. A diagram of a typical system using interleaving is shown in Figure 2.4.
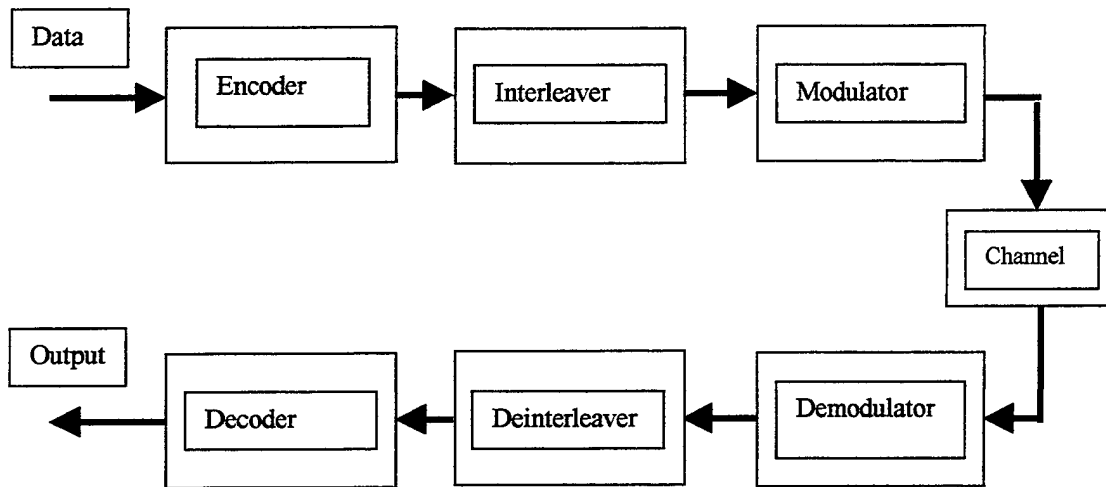
Figure 2.4. Block diagram of a communications system using Interleaving.

The ability of a block FEC code to correct errors is effectively measured by its minimum distance, and for a convolutional code, the free distance. Each serves as a figure of merit related to the number of errors that can corrected. The use of an interleaver can produce an additional decibel of coding gain [Ref. 5].

An essential and unavoidable consequence to using FECs is that the data rate is reduced by a factor equal to the code rate. Conversely, the bandwidth expansion factor is equal to $\dfrac{1}{r_c}$. In practice, this means the cost of coding gain is either an increase in bandwidth or a reduction in bit rate.

1. Convolutional Coding

Convolutional codes are produced when the information sequence is passed through a linear finite state machine. These codes can by classified as systematic or non-systematic codes. Systematic codes are non-catastrophic, meaning a finite number of errors will not result in infinite coding errors. Non-systematic codes possess larger free distances than systematic codes [Ref. 5].

Free distance is defined as the minimum distance between any two coded sequences. When using a state diagram, free distance is also defined as the weight of the minimum weight path of all possible paths that leave and then return to the all-zero state. The free distance of a convolutional code is a very effective figure of merit. It indicates the code's ability to mitigate channel noise. Non-systematic codes are used more extensively than systematic codes since non-systematic codes have larger free distances.

The constraint length (υ) of a convolutional code is the maximum number of shifts over which a single information bit can affect the output. The constraint length can greatly determine the free distance of the code and is a very important coding parameter. A large constraint length will result in a larger free distance, but will also require more decoding complexity.

Convolutional codes offer a multi-carrier system several advantages over other types of FEC codes. Convolutional codes are linear, binary, and can be represented with state diagram models or signal flow graphs. The convolutional hardware consists primarily of shift registers, which provide ease of encoding implementation.

Soft decision, Viterbi decoding is often employed. Soft decision decoding implies that the decoder uses the analog output of the demodulator. Numerical analysis

and comparison of hard decision and soft decision performance reveals that an additional

two dB of gain can be achieved using soft decision decoding [Ref. 2].

The decoder is the principal limitation of the practical application of a

convolutional system. The forward link decoder resides with the mobile. The Veterbi

soft decision decoder complexity increases exponentially as constraint length increases

[Ref. 5]. Hence, the constraint length used for the forward link is limited by the

complexity of the decoder that can be used in the mobile.

The great disadvantage to using FECs is the additional bandwidth required by the

code. This additional bandwidth lowers the potential data rate the system can achieve.

Without the additional coding gain provided by an FEC, the forward link cannot meet the

probability of bit error performance requirement of 10^{-5}. Interleaving can provide an

additional performance improvement to combat burst errors. Soft decision decoding

outperforms hard decision decoding by two dB. Given the potential coding gain, ease of

implementation, and error correcting ability, the convolutional code using soft decision

Viterbi algorithm decoding and interleaving is selected for the forward link.

D.   UPPER BOUNDED PROBABILITY OF ERROR USING CONVOLUTIONAL CODING WITH SOFT DECISION VITERBI DECODING

The probability of bit error can be upper bounded using information provided by

the code trellis. When an incorrect path is selected, the associated information bits are

decoded incorrectly. This is known as an event error. The event error occurs when the

correct path through the trellis has been eliminated in favor of an incorrect path for the

first time. Any additional errors will affect the outcome in one of three ways. Another

error can occur causing additional bit errors. The error event can result in a new path that

27

may eliminate the previous event error, hence reducing the number of bit errors. Or a new error event can partially replace the original error path, again reducing the number of errors. The probability of an error is upper bounded by the probability of a first error event. The probability of bit error is bounded by summing over all possible Hamming distances between code words [Ref. 2]:

$$P_b < \frac{1}{k} \sum_{d=d_{free}}^{\infty} \beta_d P_d \qquad (2.12)$$

where k is the number of information data bits accepted by the convolutional encoder and results in n coded bits transmitted at the output. The likelihood of selecting a code sequence that is a Hamming distance d away from the correct sequence is defined as P_d. The sum of all possible bit errors that can occur when a code sequence a distance d from the correct sequence is chosen is represented by β_d. In order to simplify the bit error calculation with only a small sacrifice in accuracy, a truncated series representing the first five terms in the series is used to approximate the complete series when $P_b \ll 1$.

The probability of selecting a code word that is a Hamming distance d away from the correct code word P_d is different for hard and soft decision decoding. The task at hand is to find P_d for BPSK with convolutional coding in a Rayleigh fading channel.

E.   UPPER BOUNDED PERFORMANCE OF BPSK WITH CONVOLUTIONAL CODING USING SOFT DECISION VITERBI DECODING IN A RAYLEIGH CHANNEL WITH FIRST TIER OMNI-DIRECTIONAL INTERFERENCE

The probability of selecting a code sequence a distance d from the correct code sequence is equivalent to the probability of bit error with d-fold diversity. For flat, slowly fading Rayleigh channels and BPSK modulation, P_d can be shown to be [Ref. 2]:

$$P_d = \left[\frac{1}{2}(1-\mu)\right]^d \sum_{k=0}^{d-1}\binom{d-1+k}{k}\left[\frac{1}{2}(1+\mu)\right]^k \qquad (2.13)$$

$$\mu = \sqrt{\frac{\overline{\gamma_c}}{1+\overline{\gamma_c}}} \qquad (2.14)$$

where $\overline{\gamma_c}$ is the average SNR ratio per diversity channel and $\overline{\gamma_b} = d\overline{\gamma_c}$ [Ref. 2].

For general spreading codes, the average channel SNR is [Ref. 6]

$$\overline{\gamma_c} = \frac{\dfrac{1}{2}}{\dfrac{K_b-1}{3N}+\dfrac{1}{2r_c}\left(\dfrac{E_b}{N_o}\right)^{-1}+\dfrac{1}{2}\left(\dfrac{S}{\eta}\right)^{-1}} \qquad (2.15)$$

where K_b is equal to the number of users in the cell, r_c is the convolutional code rate, N is the number of chips per bit, $\dfrac{E_b}{N_o}$ is the signal-to-thermal noise ratio, and $\dfrac{S}{\eta}$ is the signal-to-first tier co-channel interference ratio. We assume that due to proper cell design that the second tier co-channel interference is negligible compared to the first tier co-channel interference.

29

The forward link uses Walsh Hadamard functions to spread the base station-to-mobile signals. Unlike a PN sequence, these functions are completely orthogonal to each other and provide orthogonal channelization for each base station-to-user signal. The high power forward link pilot tone provides each user a dedicated phase reference, further improving reception [Ref. 3]. Therefore, the intra-cell, multiuser interference term of Equation 2.15 is ideally zero.

Hence, the average channel SNR simplifies to [Ref. 6]

$$\overline{\gamma}_c = \frac{\dfrac{1}{2}}{\dfrac{1}{2r_c}\left(\dfrac{E_b}{N_o}\right)^{-1} + \dfrac{1}{2}\left(\dfrac{S}{\eta}\right)^{-1}} \qquad (2.16)$$

As shown in [Ref. 6], the SNR including co-channel interference can be approximated by

$$\overline{\gamma}_c = \frac{1}{2}\left[\frac{1}{2r_c}\left(\frac{E_b}{N_o}\right)^{-1} + \sum_{i=0}^{i_o}\left(\frac{1}{3N}\right)\left(\sum_{k=1}^{k_i}\frac{P_{ik}}{P_o}\right)\right]^{-1} \qquad (2.17)$$

The second term in 2.17 represents the multi-user co-channel interference in the first tier.

The outer summation $\displaystyle\sum_{i=0}^{i_o}\frac{1}{3N}$ is the sum of all the base stations in the first tier cells. The total number of first tier base stations is i_o. The processing gain is N. The inner

summation $\left(\displaystyle\sum_{k=1}^{k_i}\frac{P_{ik}}{P_o}\right)$ is the sum of the k_i users within the ith co-channel cell. The term

P_o represents the average power received from the reference base station, and

P_{ik} represents the average power transmitted from the ith co-channel's base station to the

k^{th} user in that co-channel cell and received at the mobile. For cells with omni-directional base station antennas, the multi-user co-channel interference term is [Ref. 6]:

$$\sum_{i=0}^{i_o}\frac{1}{3N}\left(\sum_{k=1}^{k_i}\frac{P_{ik}}{P_o}\right) = \frac{R^{n_o}}{3N}\left[k_a R^{-n_a} + k_b(2R)^{-n_b} + k_c(\sqrt{7}R)^{-n_c} + k_d(\sqrt{7}R)^{-n_d} + k_e(2R)^{-n_e} + k_f(R)^{-n_f}\right] (2.18)$$

where R is equal to the cell radius and $k_a, k_b, k_c,...$ represents the number of users each within cells, a, b, c, etc. The exponents $n_a, n_b, n_c,...$ are the path loss coefficients for cells a, b, c, etc. The term n_o represents the path loss for the reference cell.

Manipulating Equation 2.12 through Equation 2.17, we obtain the new probability of bit error.

Using the values obtained from [Ref. 7] and listed in Table 1, we plot the probability of bit error over a signal-to-noise range varying from 5 to 15. The desired performance goal is to achieve a probability of bit error less then 10^{-5} while using the smallest constraint length, processing gain, and free distance possible. The minimum processing gain necessary to maintain a probability of bit error less then 10^{-5} with six first tier co-channel cells and four users per cell is found to be thirty-two.

Constraint Length	Free Distance	β
3	5	1,4,12,32,80
5	7	4,12,20,72,225
7	10	36, 0, 211, 0, 1404·
8	10	2, 22, 60,148, 340
9	12	33,0,281,0,2179

Table 2.1. Rate ½ convolutional code parameters.

For PCS Communications, where the frequencies are between 1500 MHz and

2000 MHz, the acceptable link margin for suburban areas are 0 dB and for metropolitan

centers is 3 dB [Ref. 3]. We will assume a link margin of 2 dB.

The forward link probability of bit error for constraint lengths from six to nine

with a path loss coefficient of two is illustrated by Figure 2.5.
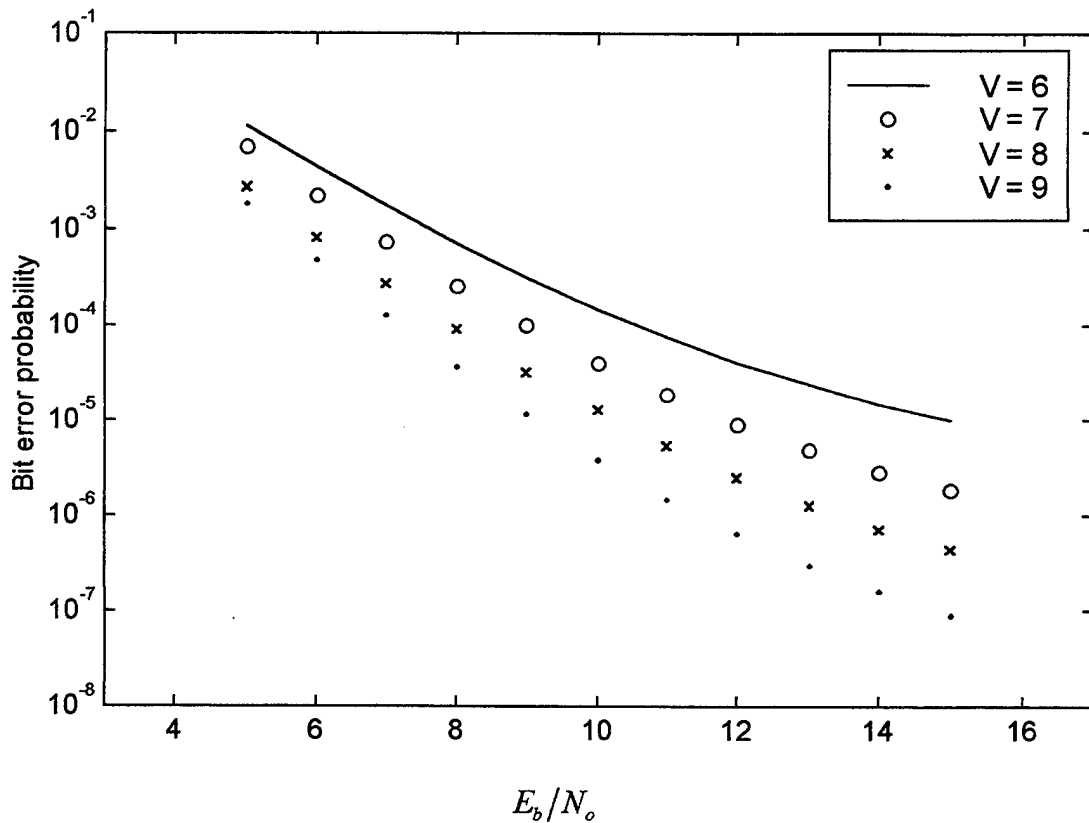
Figure 2.5. Forward link performance with an omni-directional antenna system using
a rate ½ convolutional code and soft decision decoding. Simulation parameters are
four users per cell, constraint length ranging from six to nine, processing gain of 32,
with a path loss exponent of 2.0.

As constraint length increases, the corresponding probability of bit error decreases. Performance for constraint lengths six through nine with four users and a path loss coefficient varying from 2.5 to 4.0 are plotted in Figures 2.6 through 2.9 for SNR ranging from 5 to 15.
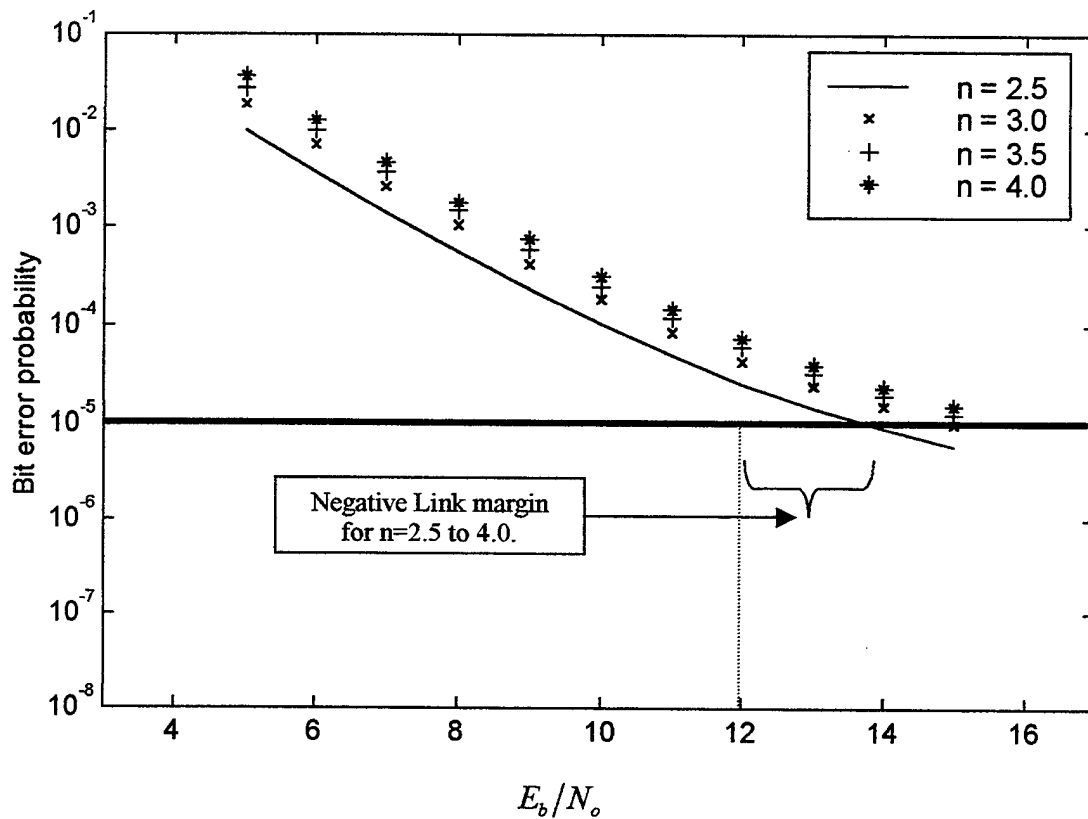
Figure 2.6. Forward link performance with an omni-directional antenna system using a rate ½ convolutional code and soft decision decoding. Simulation parameters are four users per cell, constraint length six, processing gain of 32, with path loss exponents ranging from 2.5 to 4.0.

At a signal-to-noise ratio of 12 dB, we see from Figure 2.6 that a constraint length six convolutional code does not provide sufficient link margin for our system for any reasonable value of path loss exponent.
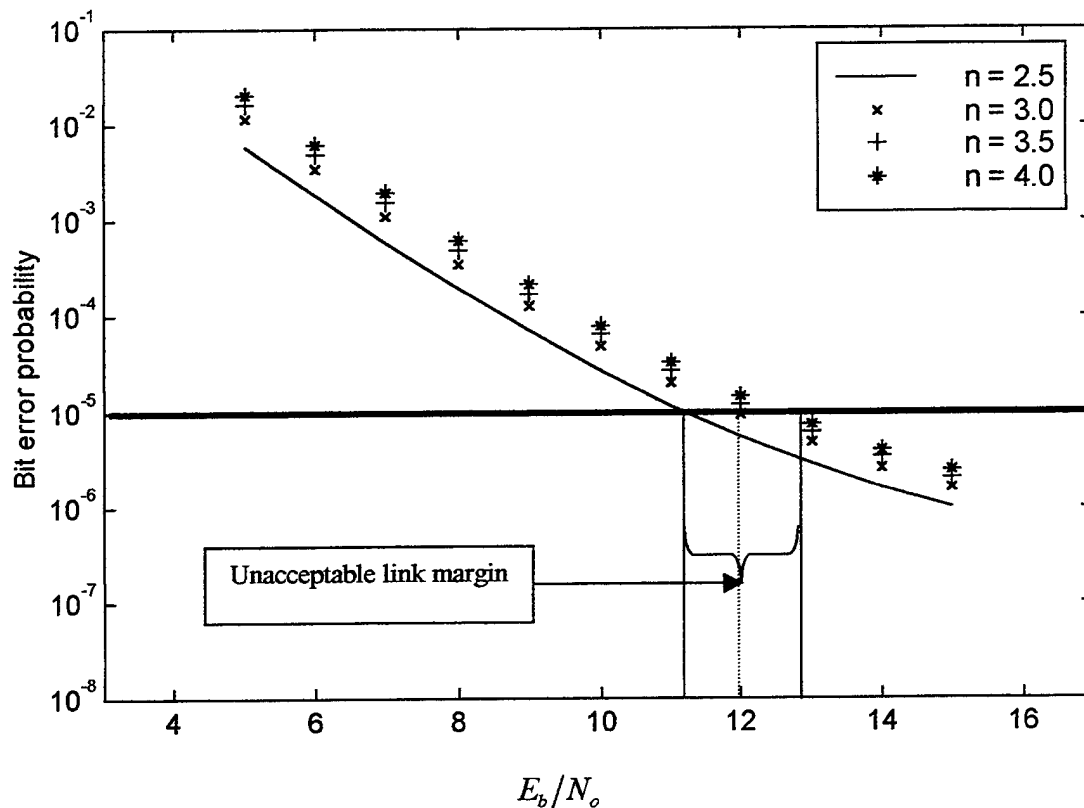
Figure 2.7. Forward link performance with an omni-directional antenna system using a rate ½ convolutional code and soft decision decoding. Simulation parameters are four users per cell, constraint length seven, processing gain of 32, with path loss exponents ranging from 2.5 to 4.0.

Changing the constraint length of the convolutional code to seven, we observe at a signal-to-noise ratio of 12 dB and a path loss exponent varying from 2.5 to 4.0 the system fails to achieve a link margin greater than 2 dB. In fact, path loss exponents of 3.5 and 4.0 result in negative link margin, where path loss exponents of 2.5 and 3.0 are positive but remain below our link margin goal of 2 dB.
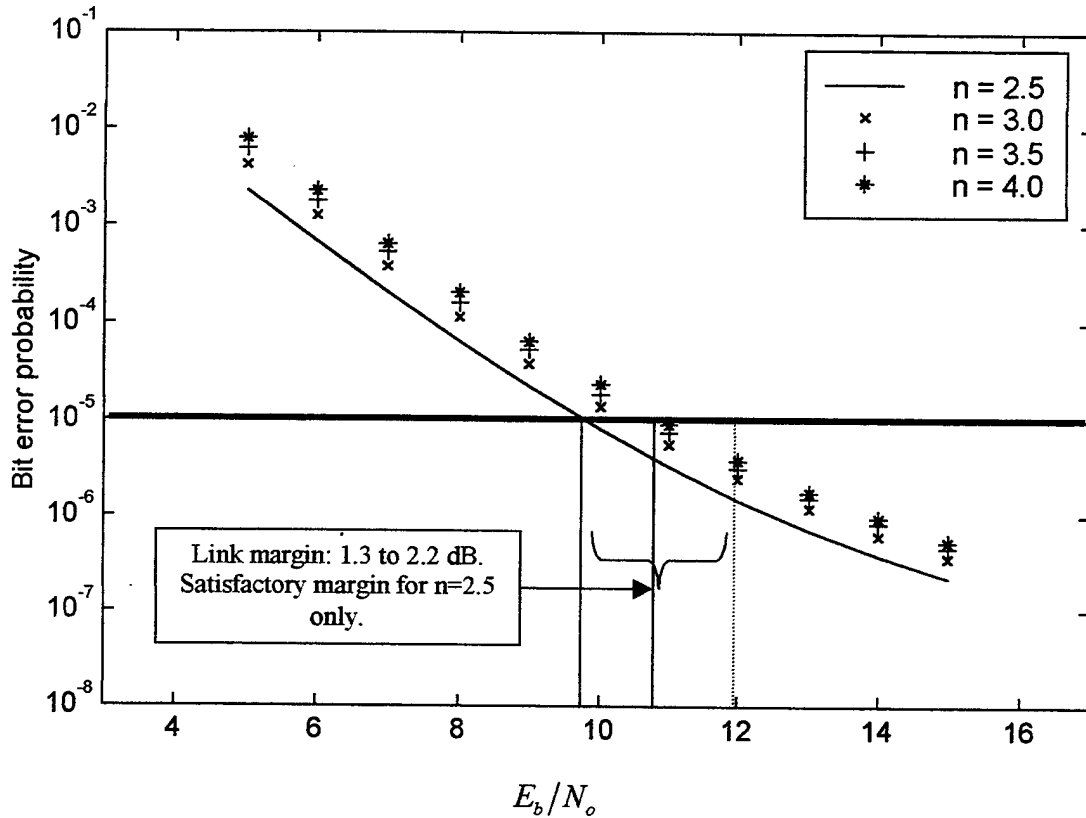
Figure 2.8. Forward link performance with an omni-directional antenna system using a rate ½ convolutional code and soft decision decoding. Simulation parameters are four users per cell, constraint length eight, processing gain of 32, with path loss exponents ranging from 2.5 to 4.0.

At an SNR of 12 dB, we see from Figure 2.8 that the convolutional code of

constraint eight provides a satisfactory link margin of 2.2 dB for a path loss

coefficient of 2.5. The path loss coefficients of 3.0, 3.5, and 4.0 do not provide a link

margin $\geq$ 2 dB.

Figure 2.9. Forward link performance with an omni-directional antenna system using a rate ½ convolutional code and soft decision decoding. Simulation parameters are four users per cell, constraint length nine, processing gain of 32, with path loss exponents ranging from 2.5 to 4.0.

With a constraint length of nine, the performance illustrated in Figure 2.9 demonstrates that the convolutional coded system provides a satisfactory link margin ranging from 2.5 to 3.2 dB for the path loss coefficients ranging from 4.0 to 2.5, respectively.

At a signal-to-noise ratio of twelve dB, we see from Figures 2.5 through 2.9 that the omni-directional forward link requires a constraint length of nine to achieve a probability of bit error $\leq 10^{-5}$ and a margin of ≥ 2 dB.

To make our PCS notebook as small as possible while maintaining a 2 dB margin and at most a $P_b \leq 10^{-5}$, we prefer to use a constraint length that is less than nine with a code rate and processing gain that provides the highest data rate possible. To meet these requirements, we will investigate the use of base station antenna sectoring.

F. UPPER BOUNDED PERFORMANCE OF BPSK WITH CONVOLUTIONAL CODING USING SOFT DECISION VITERBI DECODING IN A RAYLEIGH CHANNEL WITH FIRST TIER INTERFERENCE AND 120 DEGREE DIRECTIONAL ANTENNA SECTORING

If a single omni-directional antenna at the base station is replaced with directional antennas, co-channel interference in a cellular system can be reduced at the cost of either reduced processing gain or reduced system capacity [Ref. 3]. Alternatively, for the same co-channel interference, capacity can be tripled. Each directional antenna radiates within a specific area, and the sum of the antenna coverage areas allows 360-degree coverage. We shall analyze the probability of bit error using 120-degree antenna sectoring assuming frequency re-use.
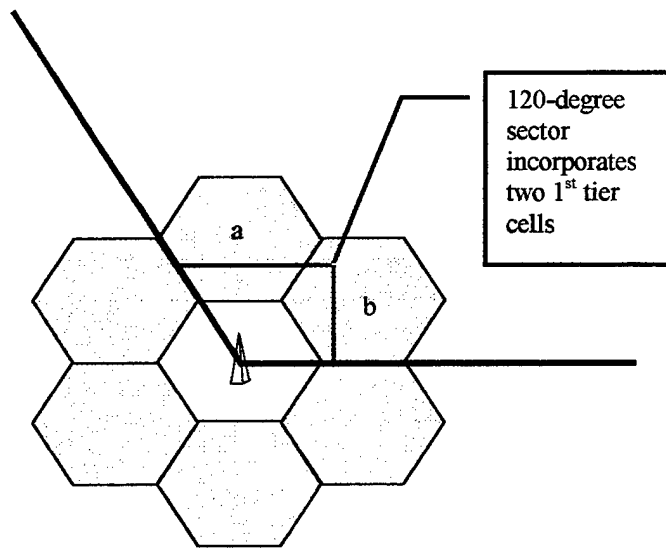
Figure 2.10. The coverage area for a 120-degree directional antenna system.

The coverage area for a 120-degree antenna is illustrated by Figure 2.10 and
reveals that two 1st tier cells are within the antenna's coverage area. For an omni-
directional antenna all six 1st tier cells are within the coverage area. To reflect the
reduction in the number of 1st tier cells affected by the base stations transmit antennas,
Equation 2.18 is replaced with [Ref. 6]

$$\sum_{i=0}^{i_o} \frac{1}{3N} \left(\sum_{k=1}^{k_i} \frac{P_{ik}}{P_o} \right) = \frac{1}{3N} \left[k_a (2R)^{-n_a} + k_b (\sqrt{7}R)^{-n_b} \right] R^{n_o} \qquad (2.19)$$

where R is the cell radius, k_a and k_b represent the number of users each within cells a
and b. The exponents n_a and n_b are the path loss coefficients for cells a and b,
respectively. The term n_o represents the path loss for the reference cell.

39

Using Equation 2.19 instead of Equation 2.18 in Equation 2.17 and proceeding as before, we obtain the new probability of bit error for 120-degree sectoring.

Using the values listed in Table 2.1, we plot the probability of bit error over a signal to noise range varying from 5 to 15 dB. The desired performance goal is to achieve a probability of bit error less then 10^{-5} with a link margin ≥ 2 dB while using the smallest constraint length possible, a processing gain of thirty-two, and four users per cell.
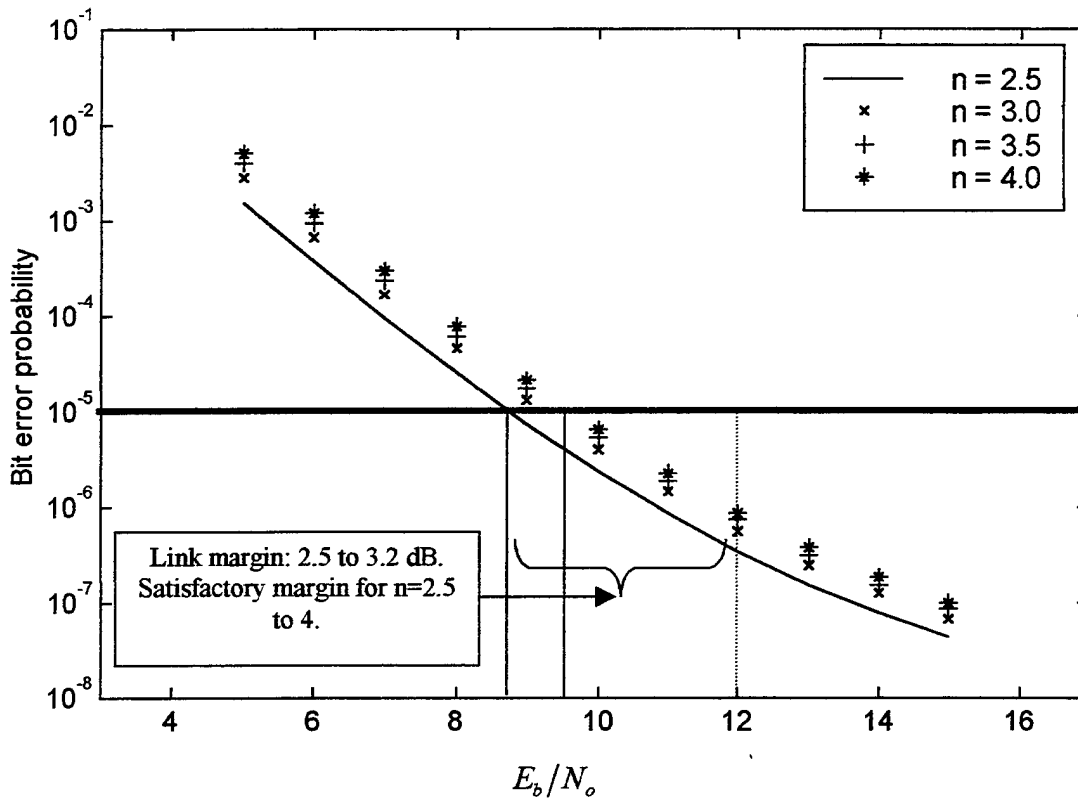
Figure 2.11. Forward link performance with an 120-degree antenna system using a rate ½ convolutional code and soft decision decoding. Simulation parameters are four users per cell, constraint length ranging from six to nine, processing gain of 32, with a path loss exponent of 2.0.

Figure 2.12. Forward link performance with a 120-degree antenna system using a rate ½ convolutional code and soft decision decoding. Simulation parameters are four users per cell, constraint length of six, processing gain of 32, with path loss exponents ranging from 2.5 to 4.0.
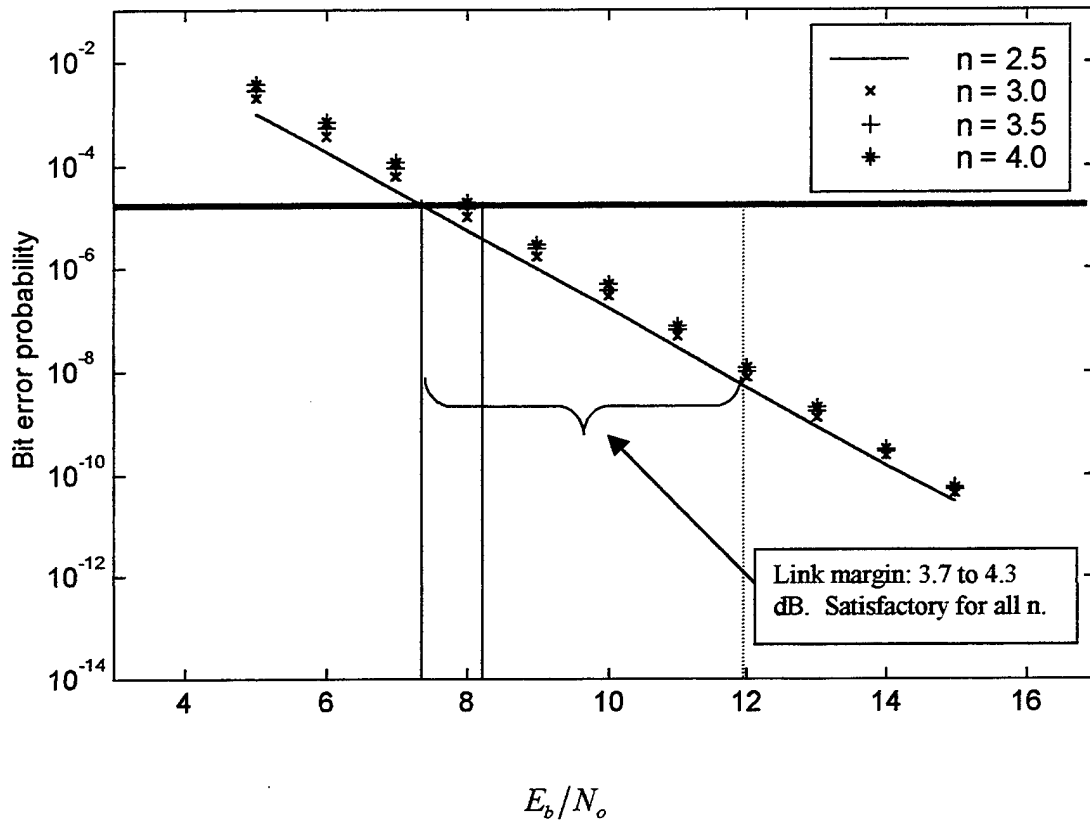
Figure 2.13. Forward link performance with a 120-degree antenna system using a rate ½ convolutional code and soft decision decoding. Simulation parameters are four users per cell, constraint length of seven, processing gain of 32, with path loss exponents ranging from 2.5 to 4.0.
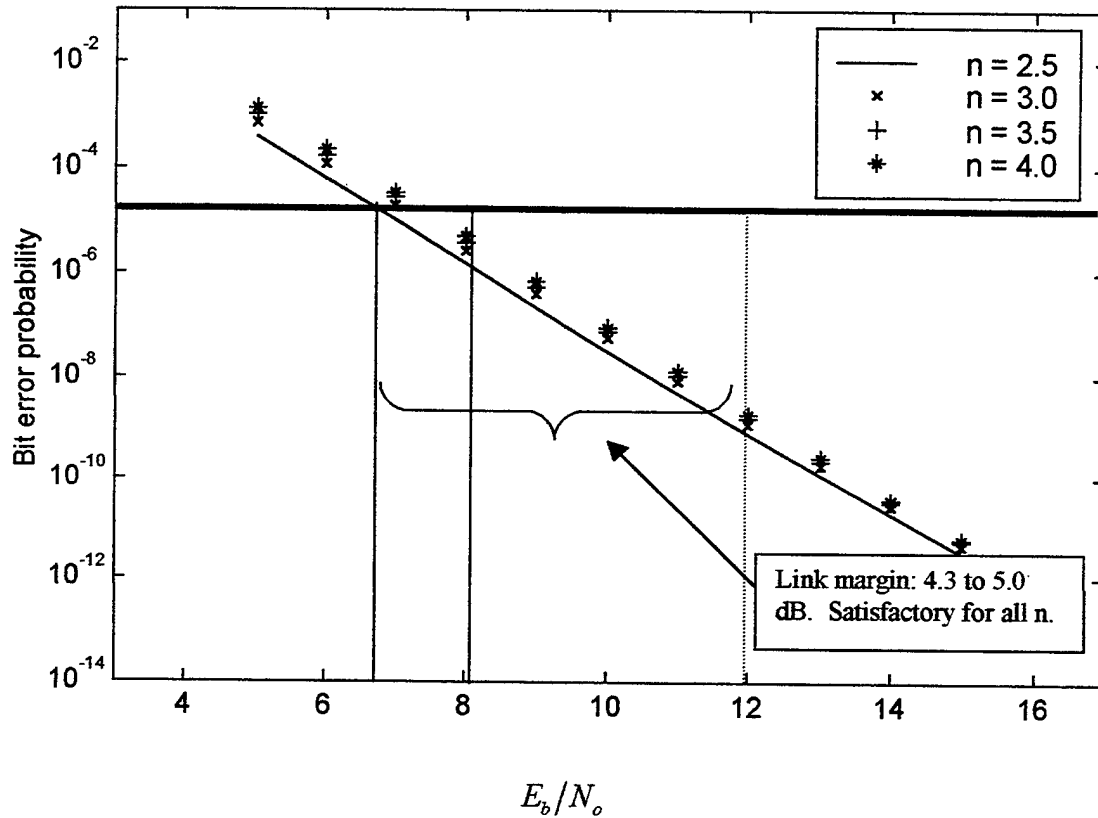
Figure 2.14. Forward link performance with a 120-degree antenna system using a rate ½ convolutional code and soft decision decoding. Simulation parameters are four users per cell, constraint length of eight, processing gain of 32, with path loss exponents ranging from 2.5 to 4.0.

Figure 2.15. Forward link performance with a 120-degree antenna system using a rate ½ convolutional code and soft decision decoding. Simulation parameters are four users per cell, constraint length of nine, processing gain of 32, with path loss exponents ranging from 2.5 to 4.0.

A rate ½ convolutional code with a constraint length ranging from six to nine, a propagation loss coefficient of two, and 120-degree sectoring yields the system probability of bit error plotted in Figure 2.11. At a signal-to-noise ratio of 12 dB, the forward link can maintain a probability of bit error less than 10^{-5} with a link margin ranging from 3.2 to 5.4 dB. Allowing the propagation loss coefficient to vary from 2.5 to 4.0, we see from Figures 2.12 through 2.15 that the forward link with 120-degree sectoring can use a constraint length ranging from six to nine to achieve a probability of bit error $\leq 10^{-5}$ with a link margin ranging from 2.6 to 5.7 dB, respectively.

Figure 2.16. Forward link performance with a 120-degree sectoring antenna system using a rate ½ convolutional code and soft decision decoding. Simulation parameters are four users per cell, constraint length six, processing gain of 16, with path loss exponents ranging from 2.5 to 4.0.
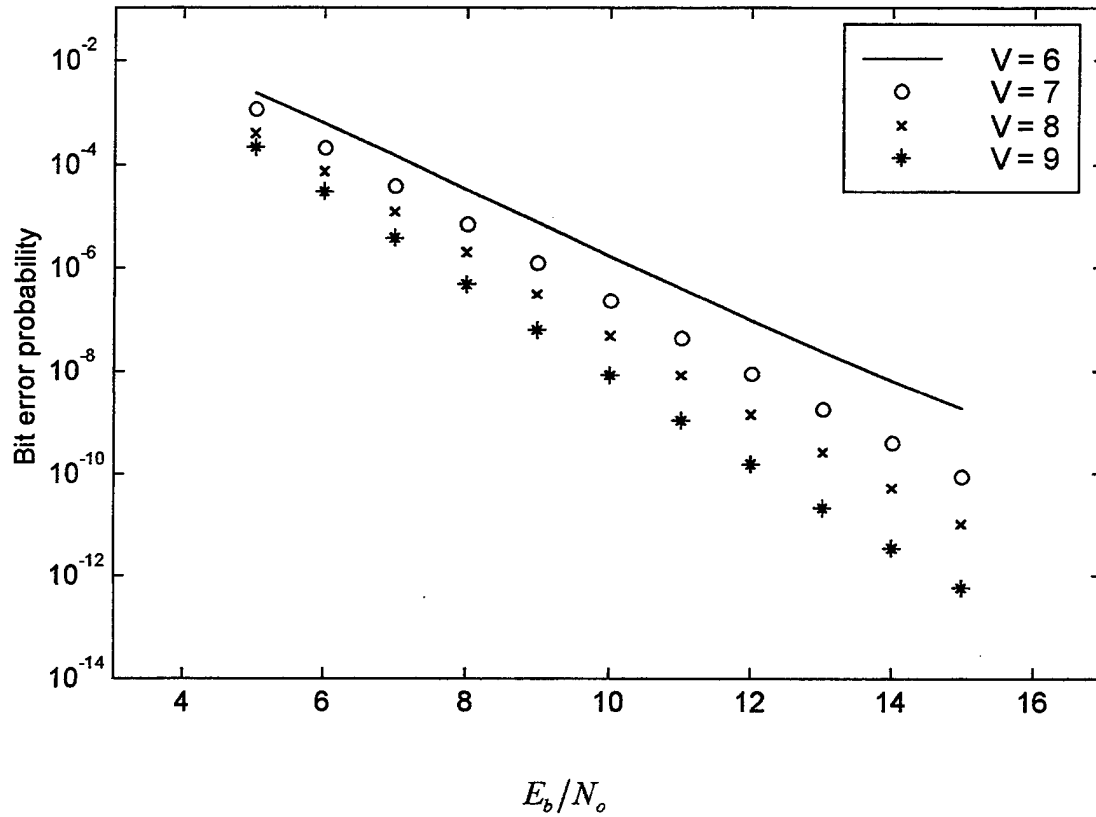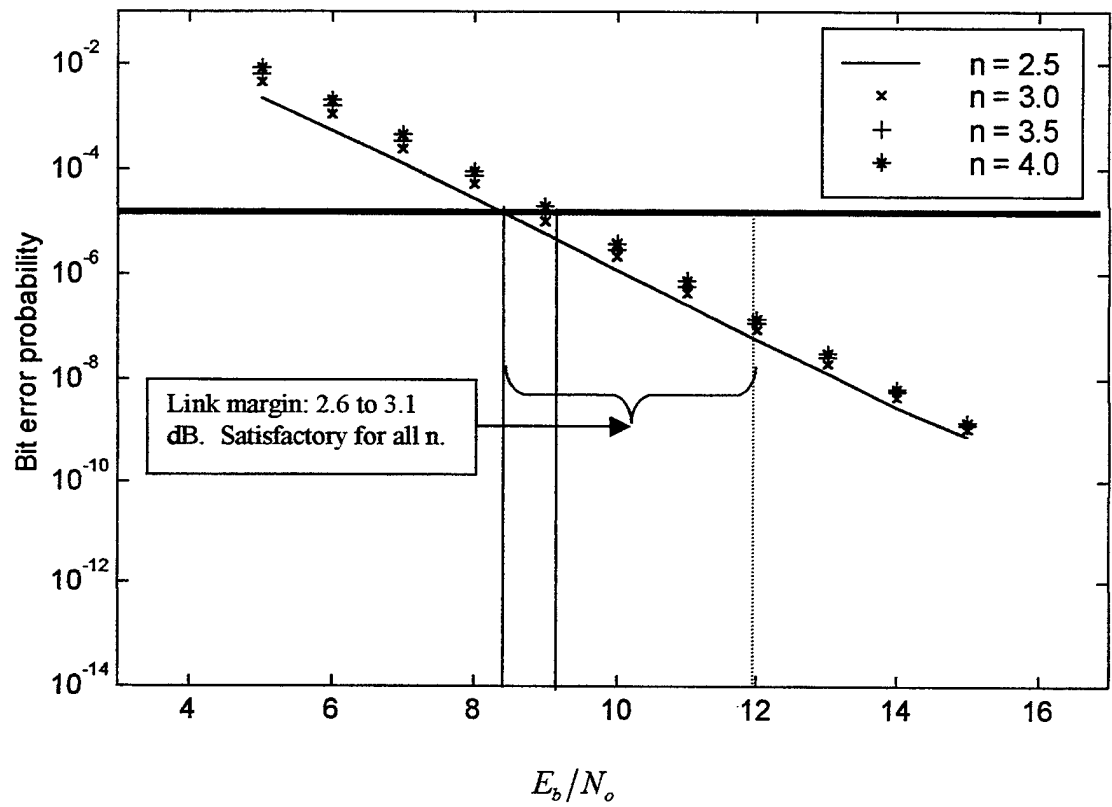
Figure 2.17. Forward link performance with a 120-degree sectoring antenna system using a rate ½ convolutional code and soft decision decoding. Simulation parameters are four users per cell, constraint length five, processing gain of 16, with path loss exponents ranging from 2.5 to 4.0.

At a signal-to-noise ratio of twelve dB, a constraint length of six, and a processing gain of 16, we see from Figure 2.16 that the forward link probability of bit error is less than 10^{-5} with a link margin ranging from 2.3 to 3.0 dB. Changing the constraint length to five, we see from Figure 2.17 that the link margin varies 1.2 and 2 dB.

Directional antenna sectoring offers significant forward link improvements. The 120-degree system allows us to reduce the constraint length from nine to six and the processing gain by a factor of two.

The 120-degree sectoring will result in a smaller PCS notebook capable of lower co-channel interference but will also reduce processing gain or system capacity. Alternatively, for the same co-channel interference, capacity can be increased. One must question whether greater systems performance can be achieved by further sectoring our base station antenna system. We will now investigate the use of 60-degree base station antenna sectoring assuming frequency re-use.

G. UPPER BOUNDED PERFORMANCE OF BPSK WITH CONVOLUTIONAL CODING USING SOFT DECISION VITERBI DECODING IN A RAYLEIGH CHANNEL WITH FIRST TIER INTERFERENCE AND 60 DEGREE DIRECTIONAL ANTENNA SECTORING

If the three 120-degree antennas at the base station are replaced with six 60-degree directional antennas, the co-channel interference in a cellular system is further reduced if we assume frequency re-use [Ref. 3]. Alternatively, for the same co-channel interference, capacity can be increased six-fold. Each directional antenna radiates within a specific area and the sum of the antenna coverage areas allows 360-degree coverage. We shall analyze the probability of bit error using 60-degree antenna sectoring assuming frequency re-use.
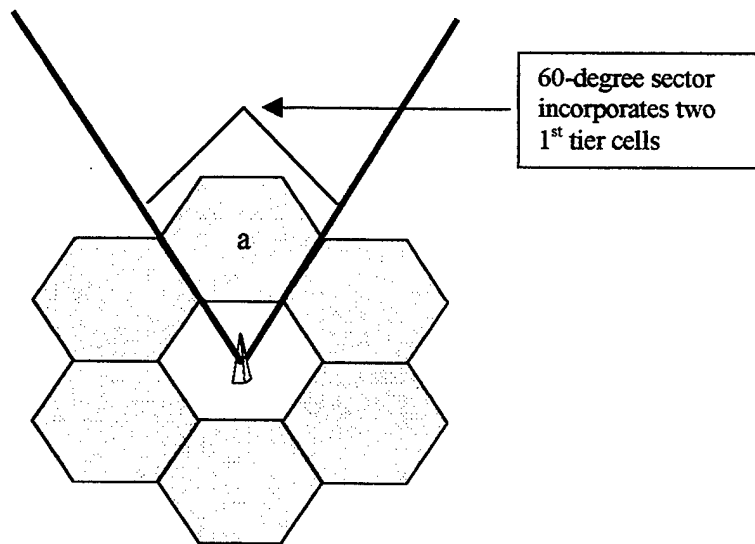
Figure 2.18. The antenna coverage area for a 60-degree directional antenna system.

The coverage area for a 60-degree antenna is illustrated by Figure 2.18 and reveals that one 1st tier cell is within the antenna's coverage area. For a 120-degree antenna, two 1st tier cells are within the coverage area. To reflect the decrease in the number of 1st tier cells affected by the base station's transmit antenna, Equation 2.18 is replaced with [Ref. 6]

$$\sum_{i=0}^{i_o} \frac{1}{3N}\left(\sum_{k=1}^{k_i} \frac{P_{ik}}{P_o}\right) = \frac{1}{3N}\left[+ k_a \left(\sqrt{7}R\right)^{-n_a}\right]R^{n_o} \tag{2.20}$$

where, again, R is the cell radius, and k_a represents the number of users each within cell a. The exponent n_a is the path loss coefficient for cell a. The term n_o represents the path loss for the reference cell. Using Equation 2.20 instead of Equation 2.19 in Equation 2.17, we obtain the new probability of bit error for 60-degree sectoring.

Using the values listed in Table 2.1, we plot the probability of bit error over a signal to noise range varying from 0 to 15 dB. The desired performance goal is to achieve a probability of bit error less then 10^{-5} with a link margin $\geq$ 2 dB while using the smallest constraint length possible, a processing gain of thirty-two or less, and four or more users per cell. The forward link probability of bit error for varying constant length six to nine with a path loss coefficient of two is illustrated by Figure 2.19.
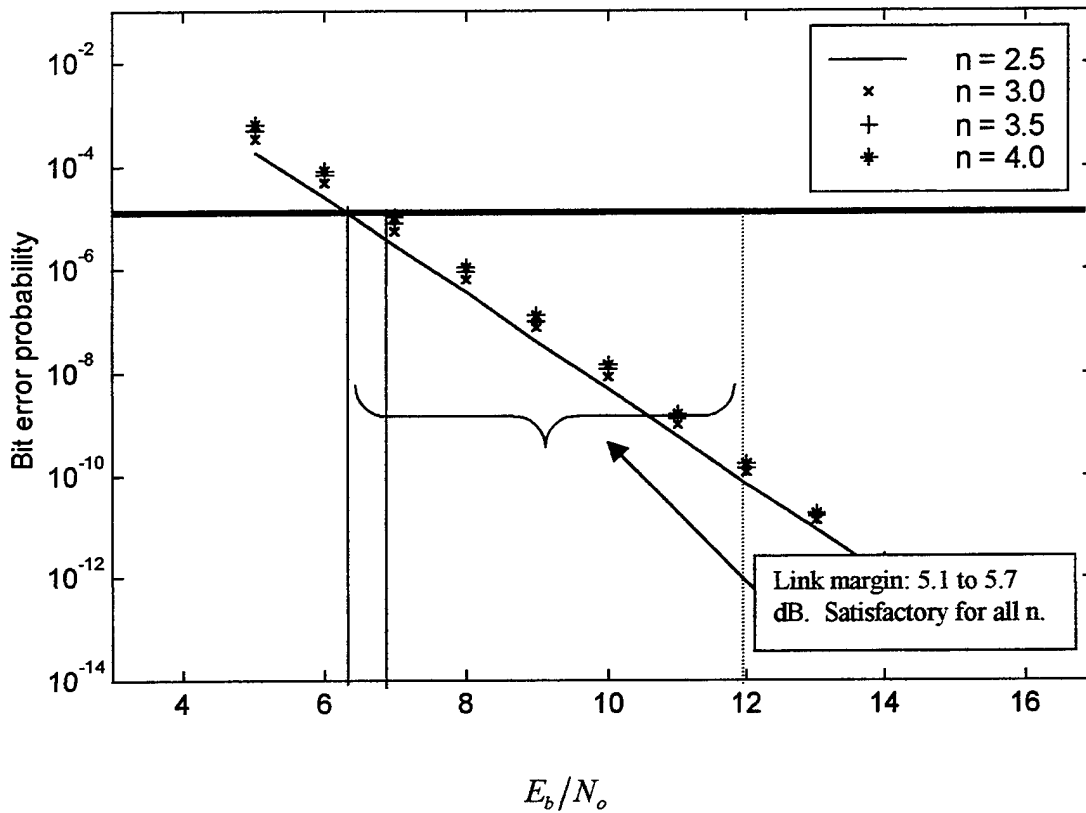
51
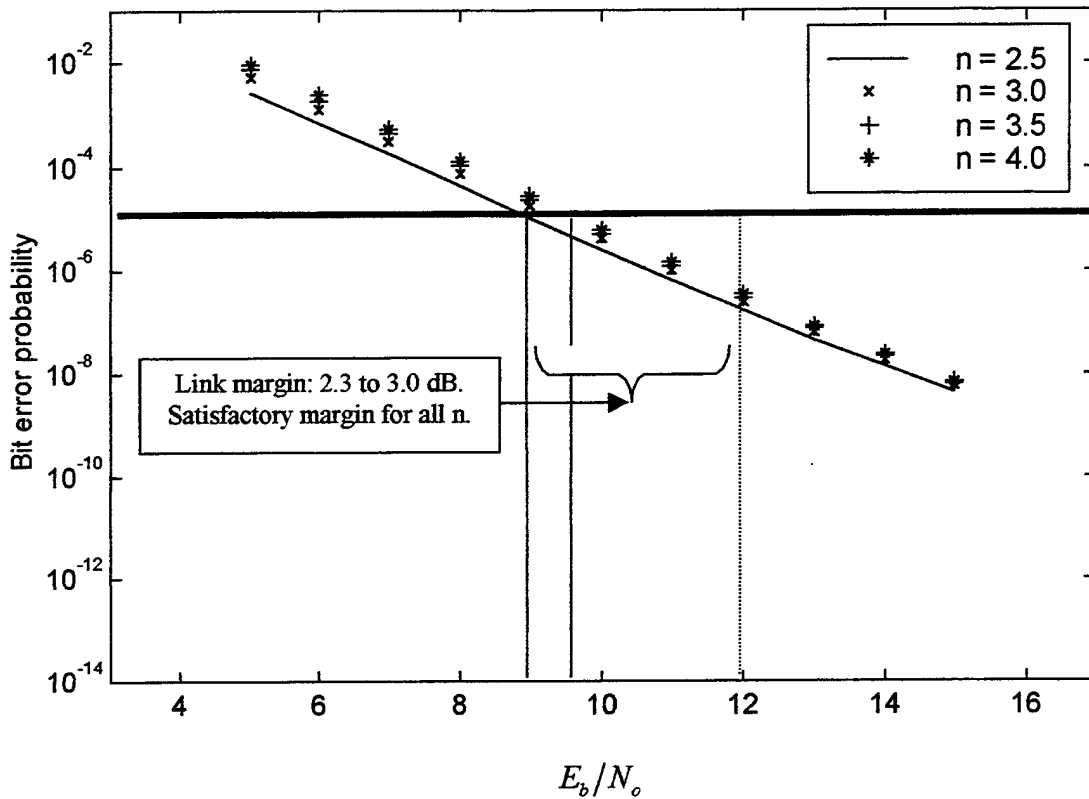
Figure 2.19. Forward link performance with a 60-degree sectoring antenna system using a rate ½ convolutional code and soft decision decoding. Simulation parameters are four users per cell, constraint length varying from six to nine, processing gain of 16, with a path loss exponent of 2.0.

Figure 2.20. Forward link performance with a 60-degree sectoring antenna system using a rate ½ convolutional code and soft decision decoding. Simulation parameters are four users per cell, constraint length of five, processing gain of 16, with path loss exponents ranging from 2.5 to 4.0.
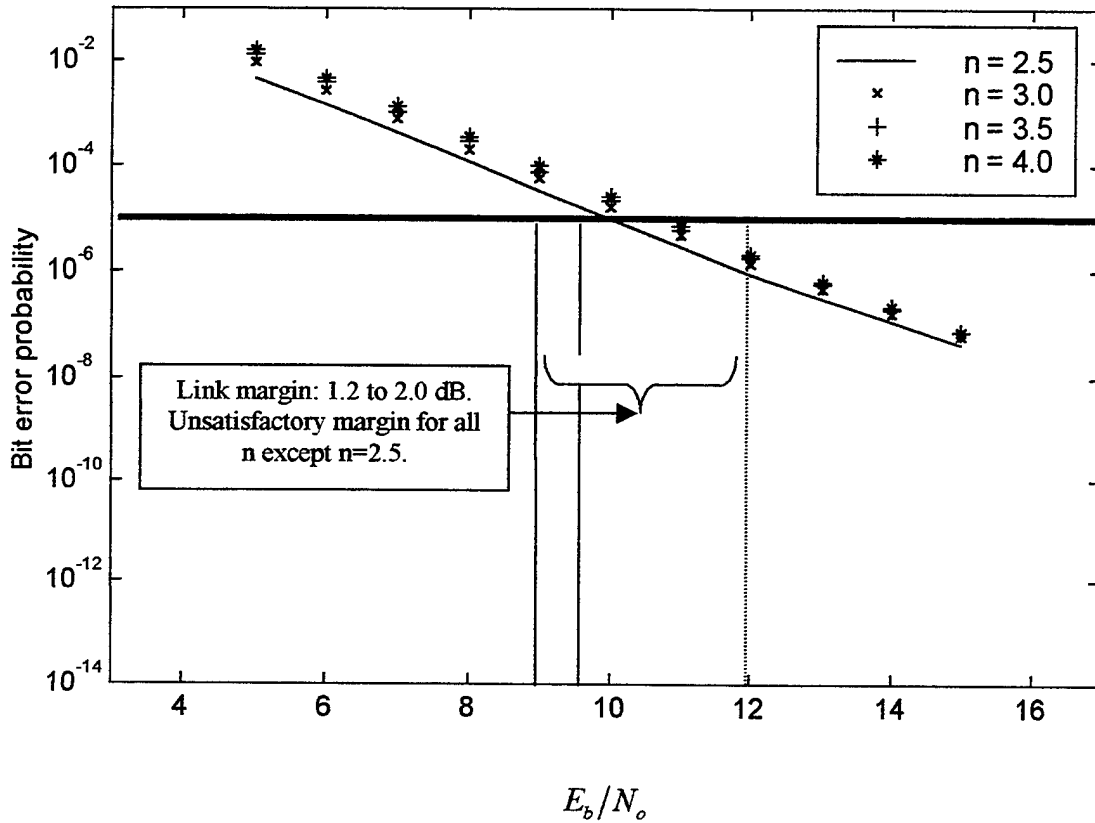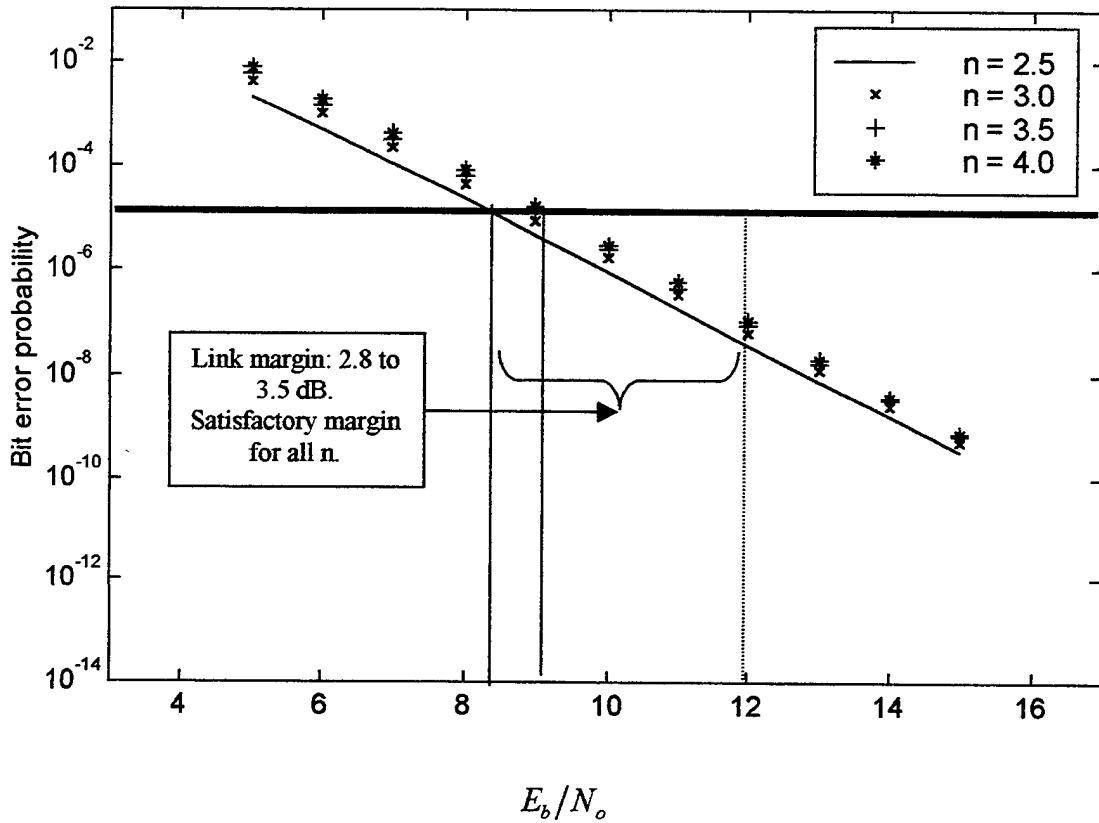
Figure 2.21. Forward link performance with a 60-degree sectoring antenna system using a rate ½ convolutional code and soft decision decoding. Simulation parameters are four users per cell, constraint length of six, processing gain of 16, with path loss exponents ranging from 2.5 to 4.0.

Figure 2.22. Forward link performance with a 60-degree sectoring antenna system using a rate ½ convolutional code and soft decision decoding. Simulation parameters are four users per cell, constraint length of seven, processing gain of 16, with path loss exponents ranging from 2.5 to 4.0.

Figure 2.23. Forward link performance with a 60-degree sectoring antenna system using a rate ½ convolutional code and soft decision decoding. Simulation parameters are four users per cell, constraint length of eight, processing gain of 16, with path loss exponents ranging from 2.5 to 4.0.

Figure 2.24. Forward link performance with a 60-degree sectoring antenna system using a rate ½ convolutional code and soft decision decoding. Simulation parameters are four users per cell, constraint length of nine, processing gain of 16, with path loss exponents ranging from 2.5 to 4.0.

To maintain a probability of bit error $\leq 10^{-5}$ and the link margin ≥ 2 dB, we see

from Figures 2.19 through 2.24 that the constraint length must be ≥ 6 for a processing

gain of 16. A constraint length six, as illustrated by figure 2.21, will meet our

performance goals and provide a link margin between 2.8 and 3.5 dB. We see from a

comparison of Figures 2.25 and 2.26 with Figures 2.20 and 2.24, respectively, that

increasing the processing gain by 3 dB results in an increase of 0.1 dB in link margin.

Figure 2.25. Forward link performance with a 60-degree sectoring antenna
system using a rate ½ convolutional code and soft decision decoding.
Simulation parameters are four users per cell, constraint length of five,
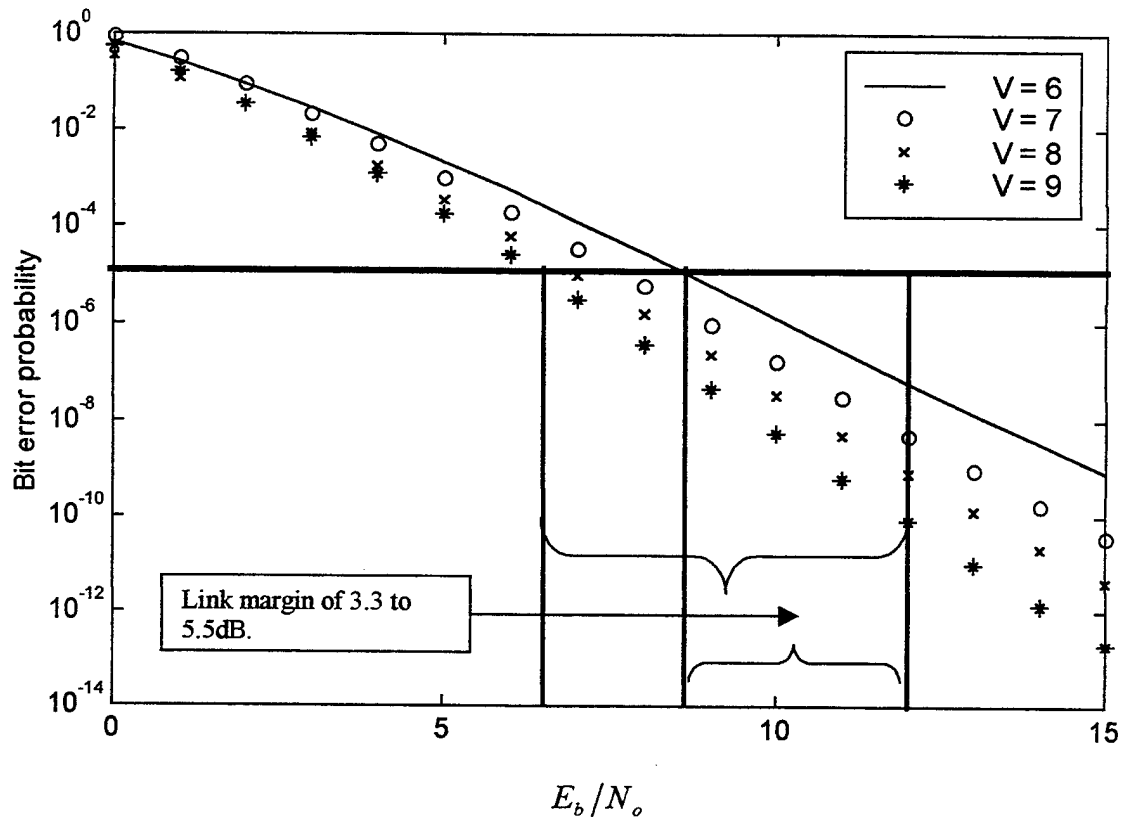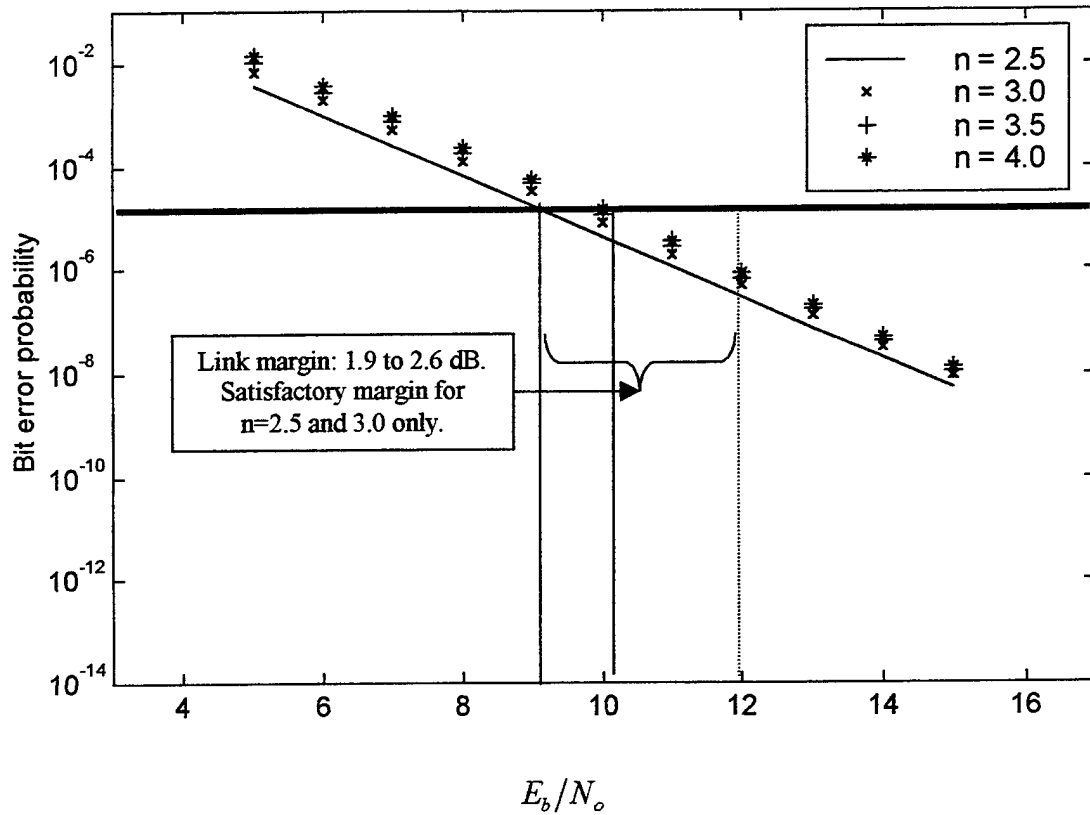processing gain of 32, with path loss exponents ranging from 2.5 to 4.0.

Figure 2.26. Forward link performance with a 60-degree sectoring antenna system using a rate ½ convolutional code and soft decision decoding. Simulation parameters are four users per cell, constraint length of nine, processing gain of 32, with path loss exponents ranging from 2.5 to 4.0.

H.   FORWARD LINK CONCLUSIONS

The analysis of the forward link requires certain key assumptions and constraints. If the modulated signal is confined to the FCC assigned bandwidth, the small physical size requirements of the mobile, the effect of fading, and multiuser interference influences our design decisions. Our established performance goals are a probability of bit error $\leq 10^{-5}$ at an SNR of 12 dB with a link margin ≥ 2 dB. The propagation coefficients used in our analysis range from 2.5 to 4.0.

To simplify our analysis, we assume the cell design is such that the second tier co-channel interference is much smaller than the first tier co-channel interference and is, therefore, negligible. The forward link uses Walsh Hadamard functions, which provides orthogonal channelization, for each base station-to-user signal. The high power forward link pilot tone improves reception by providing each user a dedicated phase reference, allowing the mobile to coherently receive the base station signal. These improvements allow us to assume that the intra-cell, multiuser interference is much smaller than the first tier co-channel interference.

Without some form of error correction, our system cannot meet established performance goals. A rate ½ convolutional code can provide sufficient error correction while constraining the signal bandwidth within the FCC guidelines.

In this chapter, seventeen different combinations of constraint length, processing gain, and antenna configurations that meet or exceed our performance goals were investigated. The simplest implementations are listed in Table 2.2

Antenna	Const. length	Processing gain	No. users	Link margin
Omni	9	32	4	2.5 dB
120	6	16	4	2.3 dB
60	6	16	4	2.8 dB

Table 2.2. Summary of forward link results.

The largest link margin obtained was 5.9 dB for 60-degree sectoring, a constraint length of 9, and a processing gain of 32. As sectoring increases, link margin also increases all other things remaining equal. Sectoring will result in a smaller PCS notebook capable of lower co-channel interference but will also reduce processing gain or system capacity. Alternatively, for the same co-channel interference, capacity can be increased.

When processing gain is increased for an omni-directional, 120-degree sectoring, or 60-degree sectoring system, we see from Figures 2.27 through 2.29 an increase in link margin. These graphs also illustrate that for lower values of SNR a difference of 3 dB in processing gain may not result in a large improvement in link margin. We also see from Figures 2.27 through 2.29 that as sectoring is increased, link margin begins to improve for larger E_b/N_o. Examining Equation 2.17, we see that the co-channel interference term is dominated by the thermal noise term until E_b/N_o becomes sufficiently large.
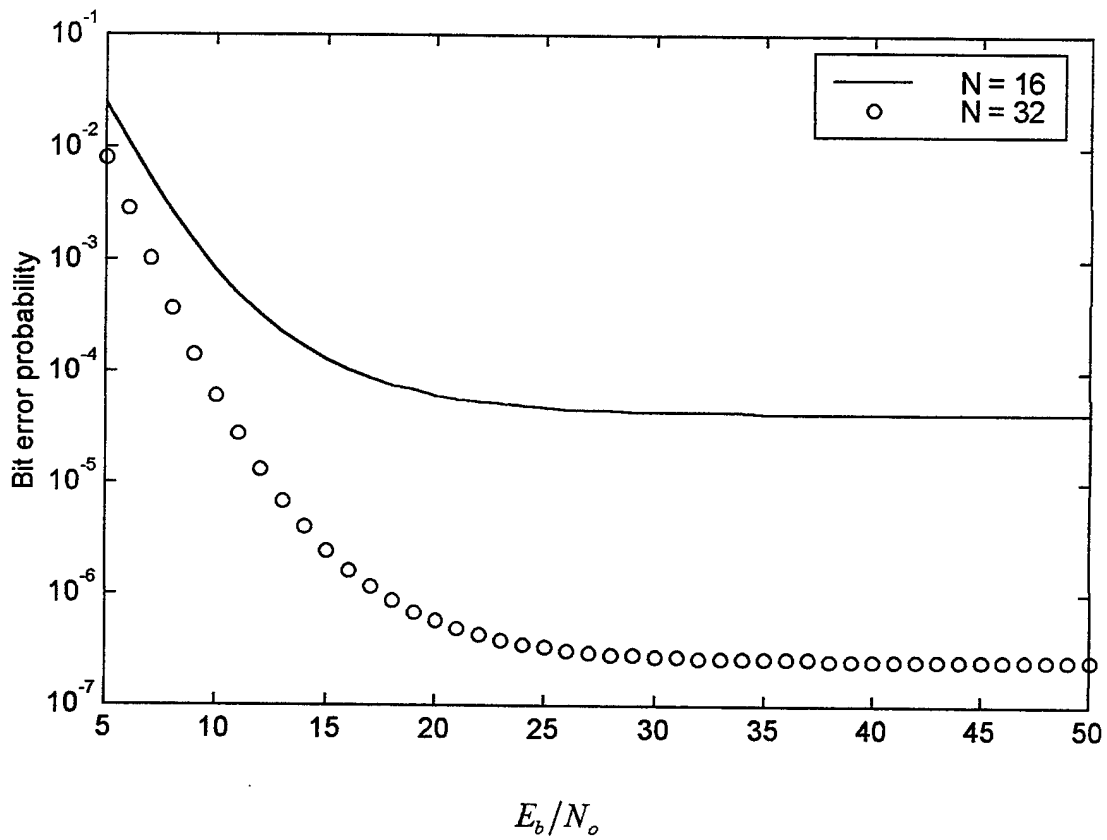
Figure 2.27. Forward link performance with an omni-directional antenna system using a rate ½ convolutional code and soft decision decoding. Simulation parameters are four users per cell, constraint length of six, processing gain of 16 and 32, with a path loss exponent of 4.0.
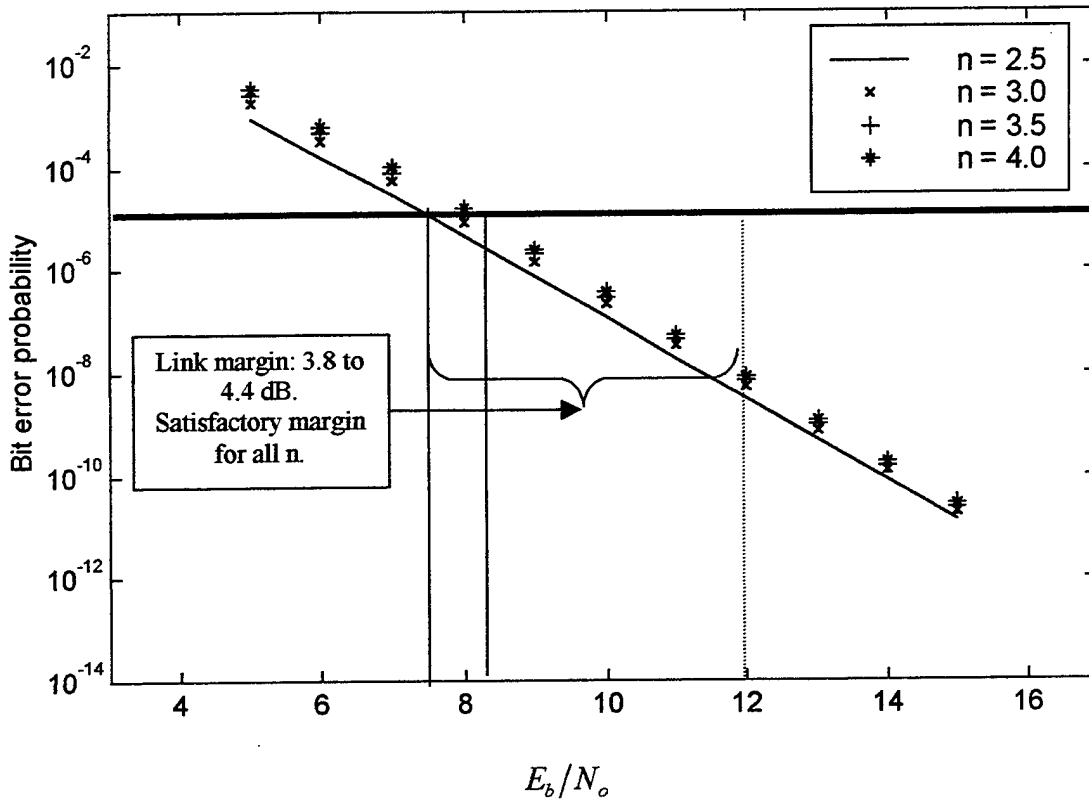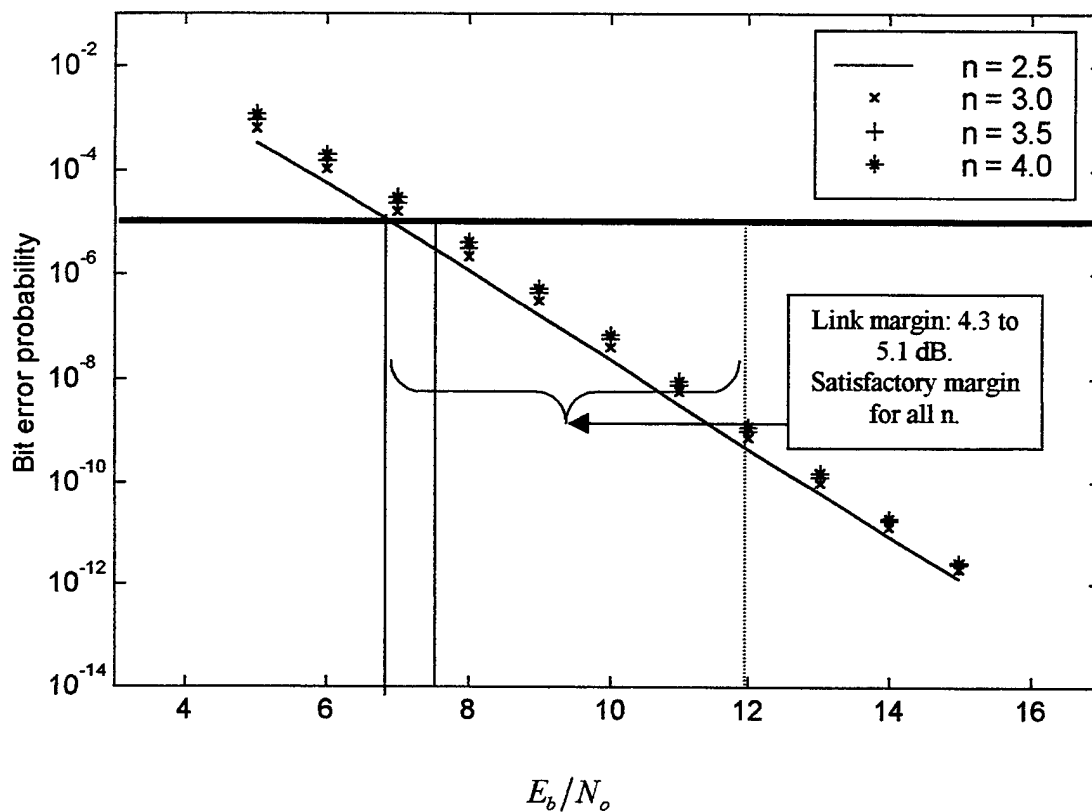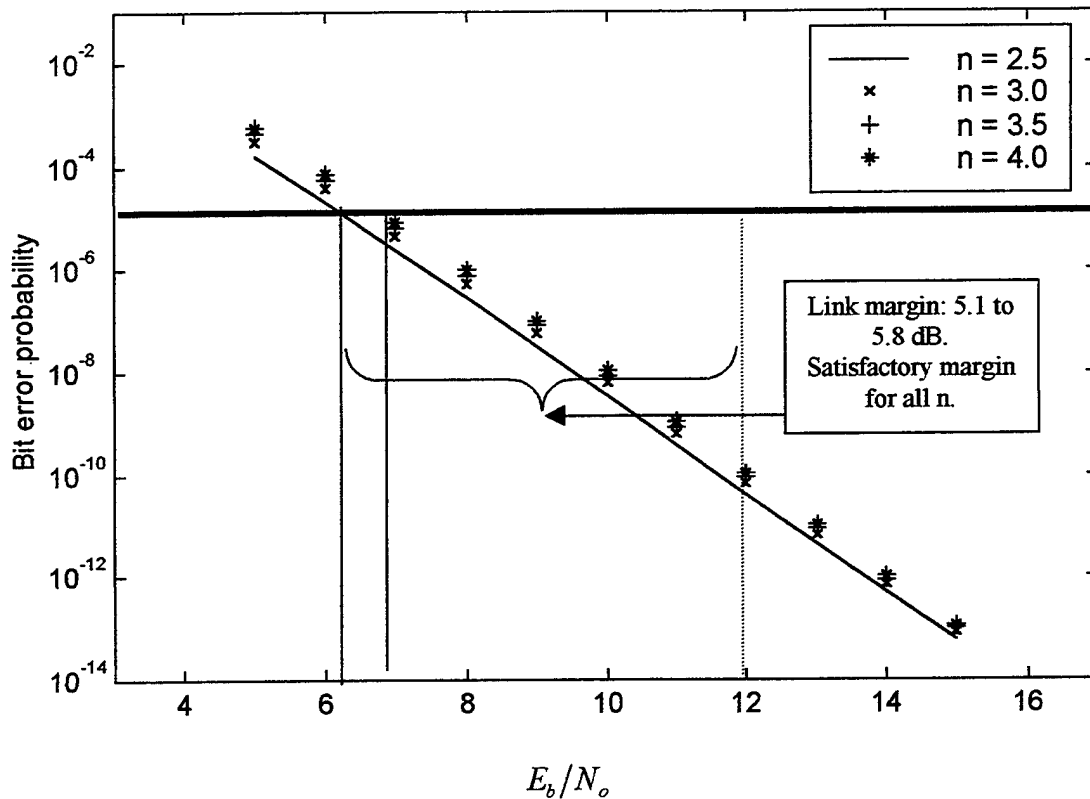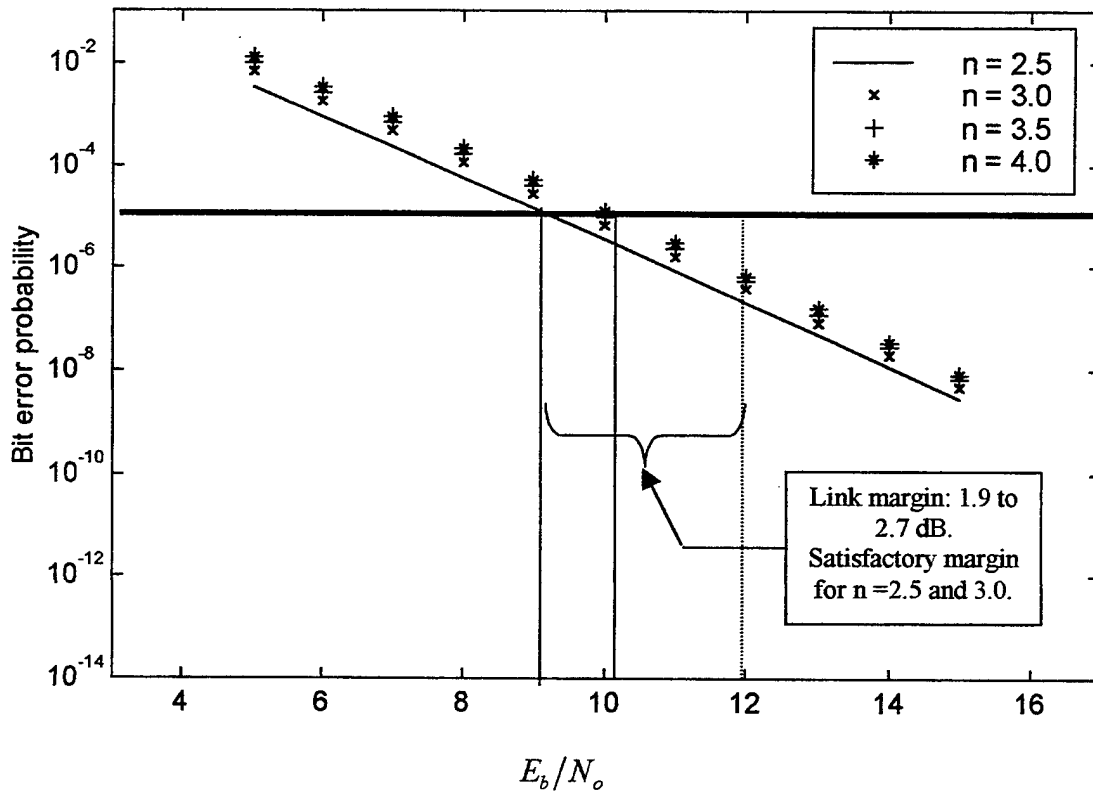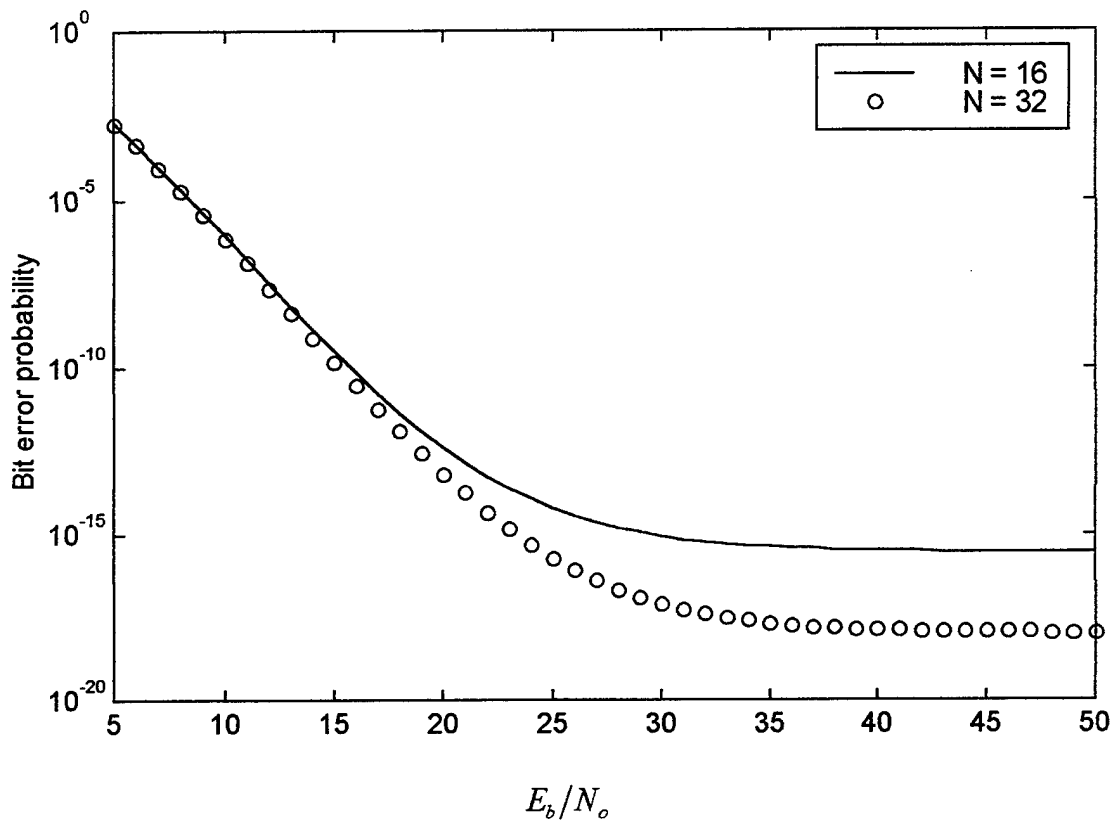
Figure 2.28. Forward link performance with a 120-degree sectoring antenna system using a rate ½ convolutional code and soft decision decoding. Simulation parameters are four users per cell, constraint length of six, processing gain of 16 and 32, with a path loss exponent of 4.0.
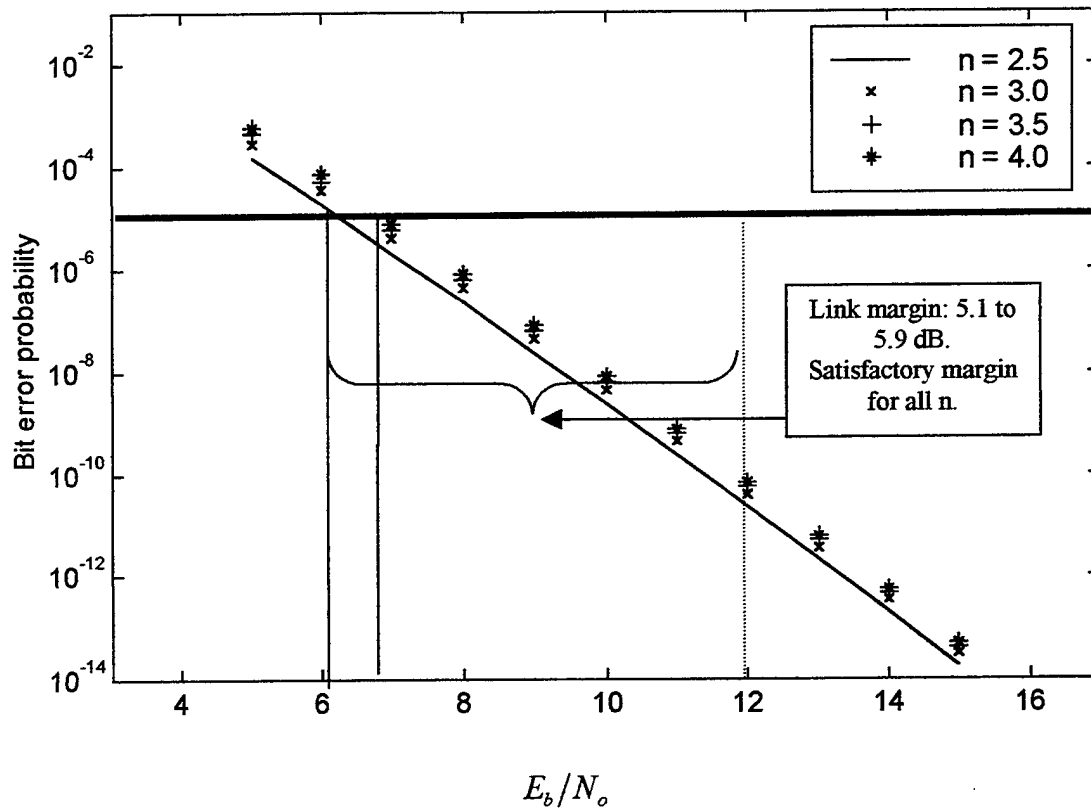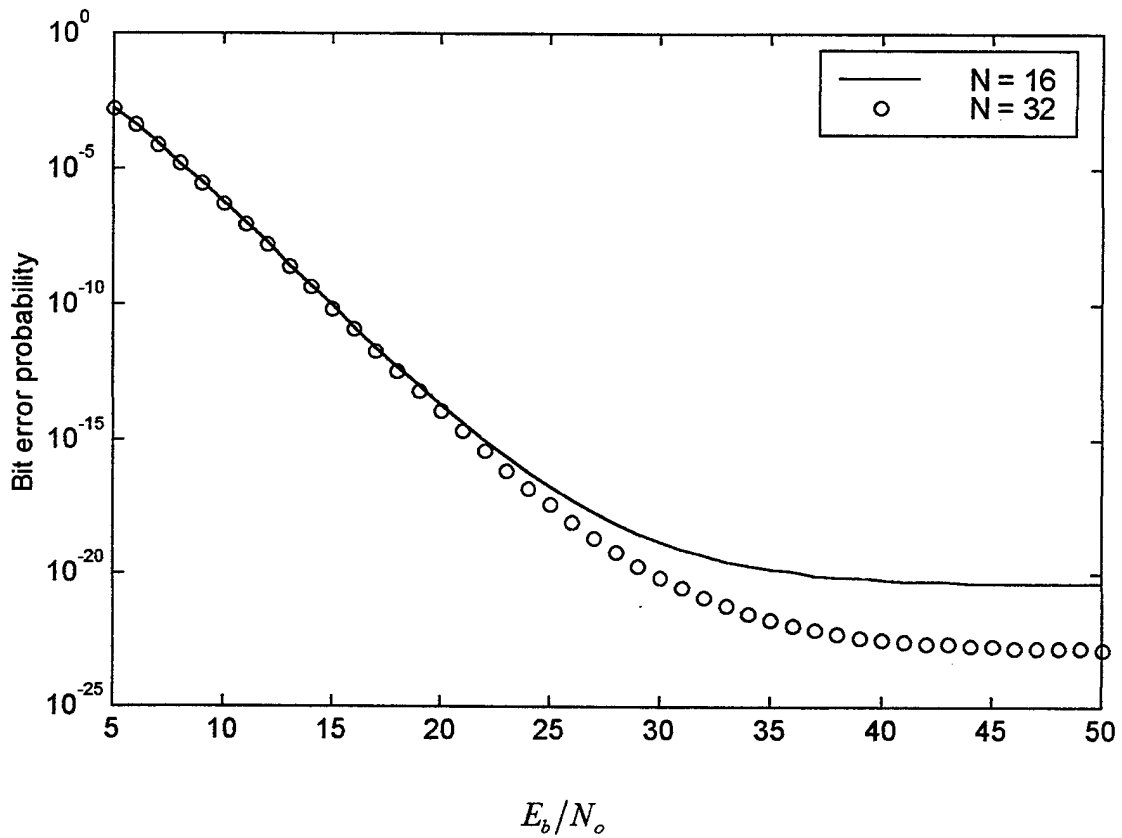
Figure 2.29. Forward link performance with a 60-degree sectoring antenna
system using a rate ½ convolutional code and soft decision decoding.
Simulation parameters are four users per cell, constraint length of six,
processing gain of 16 and 32, with a path loss exponent of 4.0.

III. ANALYSIS OF THE REVERSE LINK PERFORMANCE USING MULTICARRIER DPSK, WITH CONVOLUTIONAL CODING AND SOFT DECISION DECODING

A. MULTIPLE ACCESS AND INTERFERENCE

The system must deliver data rate on demand. As the customer requires higher data rates, the MSC will decide how many of the available carriers will be assigned to each user. This decision is based on priority and traffic intensity. As discussed in the previous chapters, the selected access technique will be code division multiple access. Unlike other multiple access techniques, a CDMA system does not separate the users with frequency or time assignments. Instead, these users are separated through the use of nearly orthogonal spreading codes.

In the case of the reverse link, the receiver is the base station and the transmitter is the user, or mobile. The maximum bandwidth available is equal to the FCC assignment of 15 MHz. For the forward link, discussed in Chapter II, the mobile applies the nearly orthogonal property of the spreading codes to recover the desired base station signal from the other unwanted signals. The reverse link uses the same property to recover the desired user from among all other users, including users from adjacent cells, as illustrated Figure 3.1. The correlation between the receiver's de-spreading code, and the unwanted user's spreading code, is ideally near zero.

Base station	⚂
User of interest within the reference cell	☺
Co-channel interference	☺
Intra-cell multi-user interference	
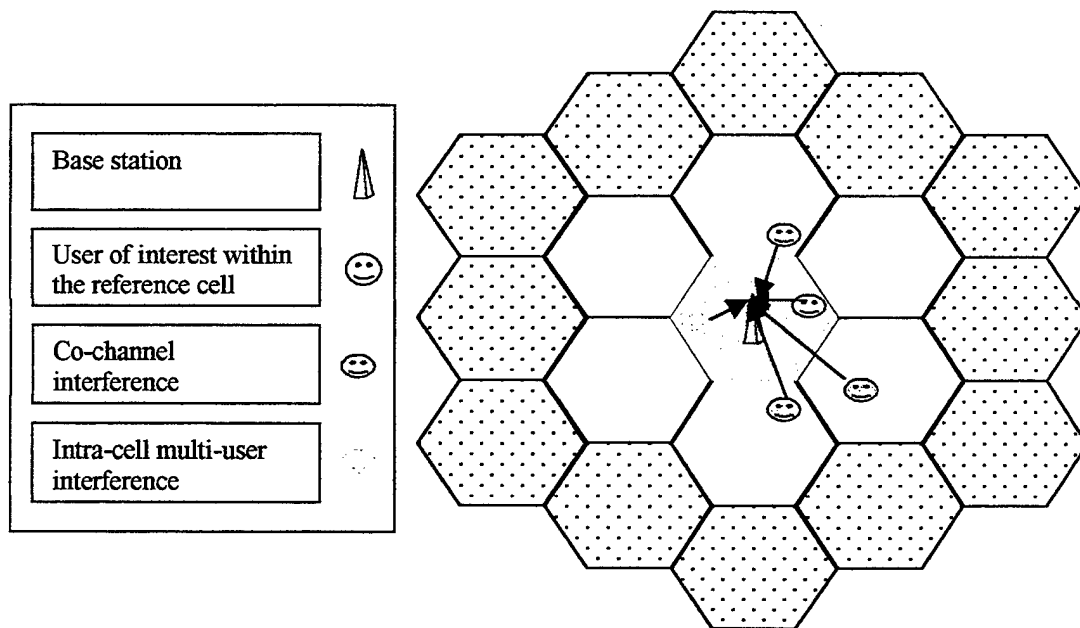
Figure 3.1. Reverse link sources of interference.

For CDMA systems, in addition to AWGN, there are primarily two forms of user generated interference. The first occurs within the cell in question, hereby referred to as the reference cell, and is the result of the additive interference of the unwanted users. This type of noise is called intra-cell multiuser interference. The second type of interference is referred to as co-channel interference and is interference that originates from the other cells instead of the reference cell. A detailed explanation of these two interference problems has been presented in Chapter II.

Given poor environmental conditions and spatial separation between cells, the co-channel interference may be so severe that several tiers of cells surrounding the reference cell may contribute to the overall co-channel interference problem. Those cells immediately around the reference cell are known as the first tier, while the second ring of

cells that surround the reference cell and the first tier cells are known as the second tier. Each may contribute to the co-channel interference problem.

The effects of co-channel interference can be reduced. Increasing the cell radius, sectoring, employing micro-zone techniques, or controlling the number of users per cell will decrease co-channel interference [Ref. 3]. Increased signal power will not reduce co-channel interference. On the contrary, power control must be used to reduce the effects of the intra-cell multi-user interference [Ref. 3]. For the purposes of this thesis, we will assume that the cell design effectively reduces the co-channel interference to the point that it is negligible compared to the multiuser interference. Therefore, the reverse link analysis will neglect co-channel interference.

B. MODULATION

Selection of the modulation technique is based on performance and system requirements. In the case of the reverse link, the user is assumed to be using a notebook size device. Physical size limits the complexity of the notebook's transmitter, which precludes the use of pilot tones. Noncoherent receivers do not require pilot tones, are easy to build, and inexpensive.

To prevent distortion, MPSK must use linear power amplifiers, while MFSK can use non-linear amplifiers. MFSK transmitters can provide higher power output signals than MPSK transmitters. MFSK can also place more power into the main lobe of the communications signal and less into the side lobes by using nonlinear amplifiers and can be received noncoherently. Only special variations of MPSK, such as differential MPSK signals, can be received noncoherently.

The most limiting factors in a broadband PCS cellular reverse link are the FCC assigned bandwidth and the physical size of the PCS notebook. As discussed in Chapter II, reverse link power control is necessary to avoid the "near-far" effect. Therefore, modulation techniques that can be implemented with low cost and small physical size are preferred.

For these reasons DPSK was chosen as the modulation technique for the reverse link. For the same probability of bit error P_b, DPSK requires three dB of signal-to-noise ratio (SNR) more than BPSK. However, the need to receive the signal noncoherently outweighs this performance difference.

C.   ANALYSIS OF DPSK IN A FREQUENCY NON-SELECTIVE SLOWLY FADING RAYLEIGH CHANNEL

For a slow, flat fading Rayleigh channel, [Ref. 2] gives the average probability of bit error for DPSK as

$$p_b = \frac{1}{2 + 2\gamma} \tag{3.1}$$

where γ is the average SNR within the channel. The average channel SNR is [Ref. 6]

$$\gamma = \frac{\frac{1}{2}}{\frac{K-1}{3N} + \frac{1}{2r_c}\left(\frac{E_b}{N_o}\right)^{-1} + \frac{1}{2}\left(\frac{S}{\eta}\right)^{-1}} \tag{3.2}$$

where K is equal to the number of users, r_c is the convolutional code rate, N is the number of chips per bit, $\frac{E_b}{N_o}$ is the signal-to-noise ratio, and $\frac{S}{\eta}$ is the signal-to-co-channel interference ratio.

For the purposes of this thesis, only the AWGN and the multiuser interference from competing users in the same cell are considered. Therefore, the average channel SNR simplifies to [Ref. 6]

$$\gamma = \frac{\dfrac{1}{2}}{\dfrac{K-1}{3N} + \dfrac{1}{2r_c}\left(\dfrac{E_b}{N_o}\right)^{-1}} \qquad (3.3)$$

1.   The Conditional Dependence of Probability of Bit Error on Number of Users

As can be seen from Equation 3.3, the average channel SNR is dependent upon $\dfrac{E_b}{N_o}$, the number of chips per bit (N), and the number of users (K) occupying each carrier. The number of chips per bit is a fixed number that will not change with time. However, each carrier can have any number of users assigned depending upon demand and traffic intensity. Therefore, the analysis must treat K as a discrete random variable. Two questions now must be answered. What distribution best represents the arrival and departure of users, and how can the probability of bit error be determined if the number of users is undergoing continuous change? The purpose of the distribution of K is to model the number of users on the system. We require a discrete distribution that can represent any positive whole number.

Unfortunately, real empirical data for broadband PCS does not exist. Therefore, some reasonable assumptions must be made with regard to the expected value of the random variable K used to model the number of users. The expected value directly determines parameters used in all discrete distributions. We will assume it is more probable that most of the users will tend to be in the center of the distribution then at the

ends. We will also assume that for the reverse link we want to provide high data rate communications for an expected value of two users. The Geometric and the Poisson distributions are the only two discrete distributions that possess the aforementioned qualities. These two distributions will now be investigated starting with the geometric distribution.

The geometric series is

$$p_K = p(1-p)^{K-1} \qquad\qquad K = 1,2,3\ldots \qquad (3.4)$$

and the expected value of K is

$$E[K] = \frac{1}{p} \qquad\qquad (3.5)$$

where the symbol p is the geometric parameter. With an expected value of two, the geometric distribution is as shown in Figure 3.2.
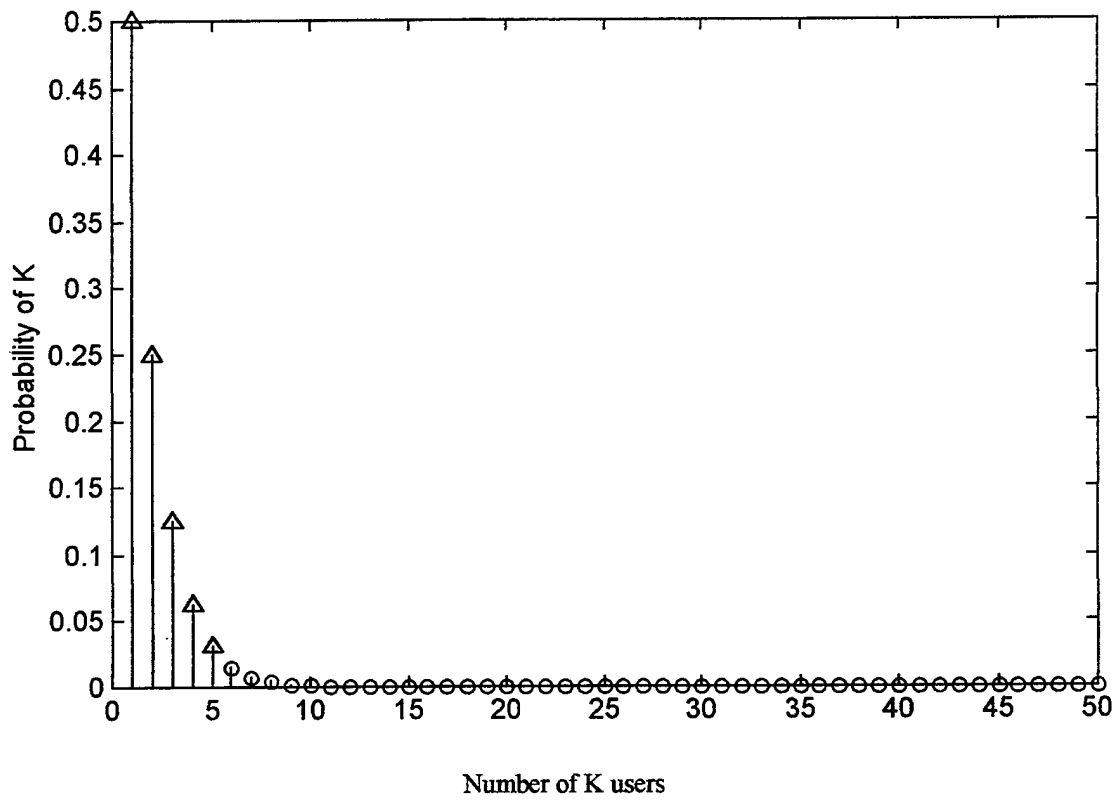
Figure 3.2. Distribution of K users as a geometric random variable with an expected value of two.

As shown in Figure 3.2, the geometric distribution assigns the higher probability to the smaller number of users. This is why the geometric distribution is known for its light traffic handling capability. This distribution gives the probability of one user occupying the carrier as $\frac{1}{2}$, the probability of two users occupying the carrier as $\frac{1}{4}$, and so on. The drawback to the geometric series from the standpoint of modeling broadband PCS is that one user is more probable then two users, which is more probable then three users, etc. A single user being the most likely does not seem to be a reasonable assumption for the envisioned broadband PCS. In order to allow two or more users to be more probable than one user, a different distribution must be used.

The Poisson distribution possesses the aforementioned characteristic. The Poisson distribution is given by

$$P_K = \left(\frac{\alpha^{K-1}}{(K-1)!} \right) e^{-\alpha} \quad K = 1, 2, 3, \ldots \tag{3.6}$$

The expected value of the random variable K is equal to the Poisson parameter α. With an expected value of two the Poisson distribution is as shown in Figure 3.3.
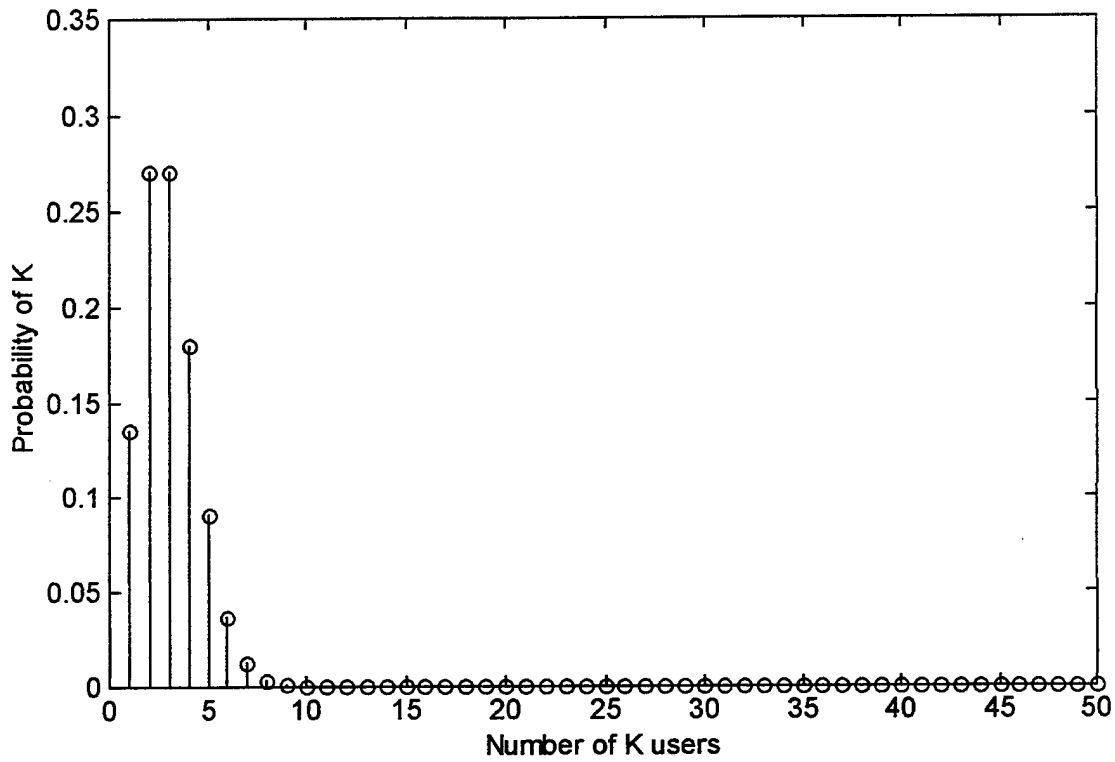
Figure 3.3. Distribution of K users as a Poisson random variable with an expected value of two.

This distribution assigns the highest probabilities to two and three users. The Poisson distribution provides us with the ability to assign the most likely number of users to be greater than one, which seems likely for broadband PCS. The geometric probability decreases as the number of users increase and the highest probability is assigned to the smallest number of users. For these reasons the Poisson distribution will be used as our distribution model.

The probability of bit error P_b is given by [Ref. 8].

$$P_b = \sum_{K=1}^{\infty} P_b(K)P_K \tag{3.7}$$

where $P_b(K)$ is the probability of bit error conditioned upon the number of users and P_K is given by Equation 3.6. The conditional probability of bit error $P_b(K)$ will be discussed in the next section.

D.   CONDITIONAL UPPER BOUNDED PROBABILITY OF ERROR USING CONVOLUTIONAL CODING WITH VITERBI SOFT DECISION DECODING IN A RAYLEIGH CHANNEL

An upper bound for the probability of bit error for binary modulation, convolutional coding with soft decision detection, and slow, flat Rayleigh fading channel is [Ref. 2].

$$P_b(K) \le \left(\frac{1}{k}\right) \sum_{d=d_{free}}^{\infty} \beta_d P_2(d) \tag{3.8}$$

where k is the number of information data bits accepted by the convolutional encoder and results in n coded bits transmitted at the output. For example, for a rate $\frac{1}{2}$ code, k is

equal to one. The sum of all possible bit errors that can occur when a code sequence a Hamming distance d from the correct code sequence is selected is represented by β_d. In order to simplify the bit error calculation with a small sacrifice in accuracy, a truncated series representing the first five terms in the series is used to approximate the complete series. The term d_{free} is the free distance of the convolutional code and is related to the constraint length of the code. The likelihood of selecting a code sequence that is a Hamming distance d away from the correct sequence is [Ref. 2].

$$P_2(d) = p_b^d \sum_{k=0}^{d-1} \binom{d-1+k}{k}(1-p_b)^k \tag{3.9}$$

The term p_b was defined in Equation 3.1. Manipulating Equations 3.1, 3.3, 3.8, and 3.9, we obtain the conditional probability of bit error.

E. UNCONDITIONAL UPPER BOUNDED PROBABILITY OF ERROR USING CONVOLUTIONAL CODING WITH VITERBI SOFT DECISION DECODING IN A RAYLEIGH FADING CHANNEL

To make practical use of Equation 3.7, the series must be truncated at some K_{max}. To determine an appropriate K_{max}, we compute Equation 3.7 for increasing K_{max} until the probability of error no longer changes. Results for K_{max} equal to 10, 20, 23, and 25 are illustrated in Figures 3.4 through 3.7.

Figure 3.4. Reverse link performance using a Poisson distribution, a rate ½ convolutional code and with soft decision decoding. Simulation parameters are ten users, constraint length nine, processing gain of 32, and Poisson parameter of two.

Figure 3.5. Reverse link performance using a Poisson distribution, a rate ½ convolutional code and with soft decision decoding. Simulation parameters are 20 users, constraint length nine, processing gain of 32, and Poisson parameter of two.

Figure 3.6. Reverse link performance using a Poisson distribution, a rate ½ convolutional code and with soft decision decoding. Simulation parameters are 23 users, constraint length nine, processing gain of 32, and Poisson parameter of two.

Figure 3.7. Reverse link performance using a Poisson distribution, a rate ½ convolutional code and with soft decision decoding. Simulation parameters are 25 users, constraint length nine, processing gain of 32, and Poisson parameter of two.

Comparing these figures, we observe that the plots remain the same for

$K_{max} \geq 23$. Hence, based on this model of broadband PCS, the possibility of more than

23 users has negligible impact on system performance.

To achieve best performance, the largest possible constraint length practical is

used. This also increases receiver complexity. Another method that improves

performance is to increase the processing gain. The disadvantage associated with

increasing processing gain is a decrease in data rate and an increase in circuitry

complexity. The plot of the upper bound of the probability of bit error for DPSK using

convolutional coding and soft decision decoding with varying constraint lengths and a

processing gain of sixteen is shown in Figure 3.8. The same plot with a processing gain

equal to thirty-two is shown in Figure 3.9.
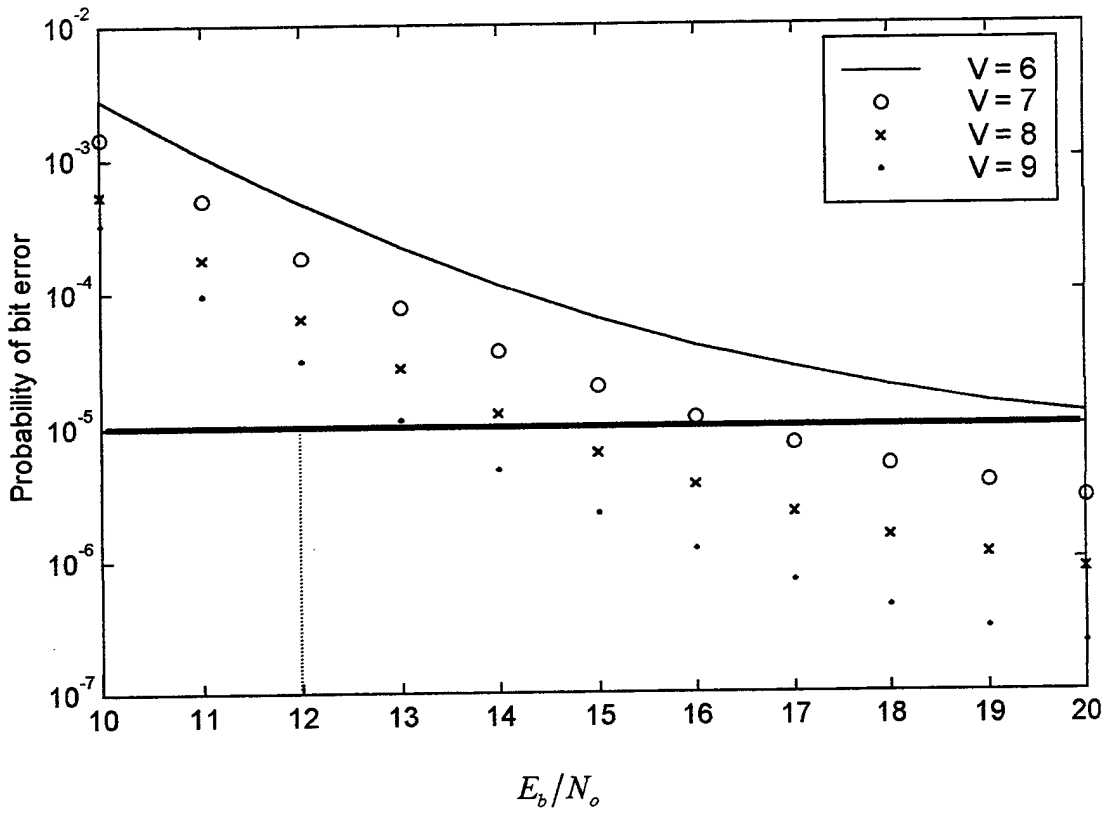
Figure 3.8. Reverse link performance using a Poisson distribution, a rate ½
convolutional code and with soft decision decoding. Simulation parameters
are 23 users, constraint length varying from six to nine, processing gain of
16, and Poisson parameter of two.
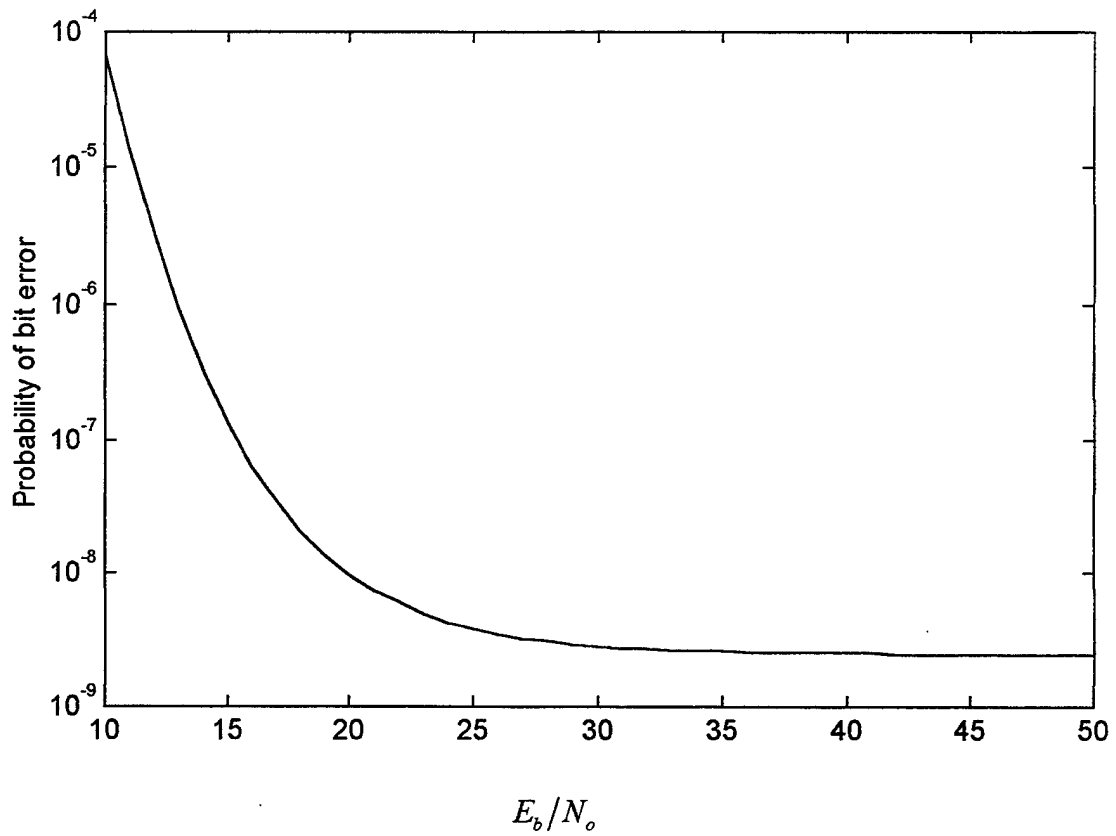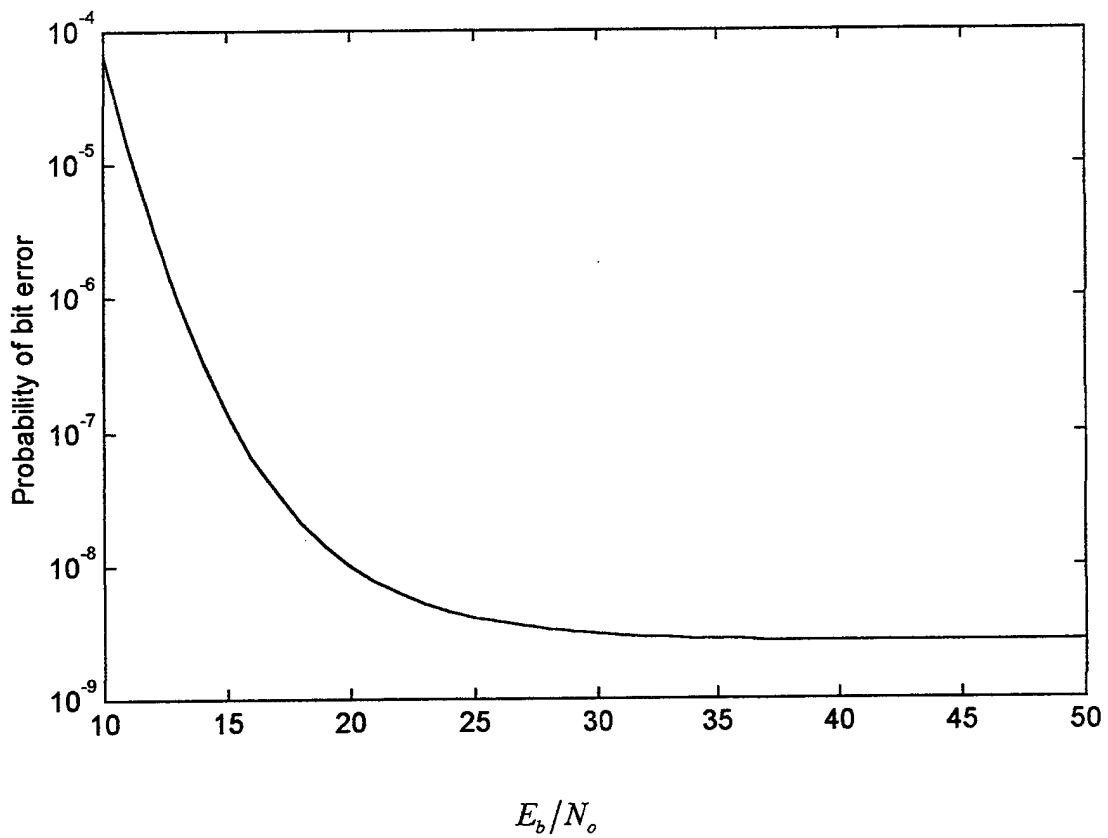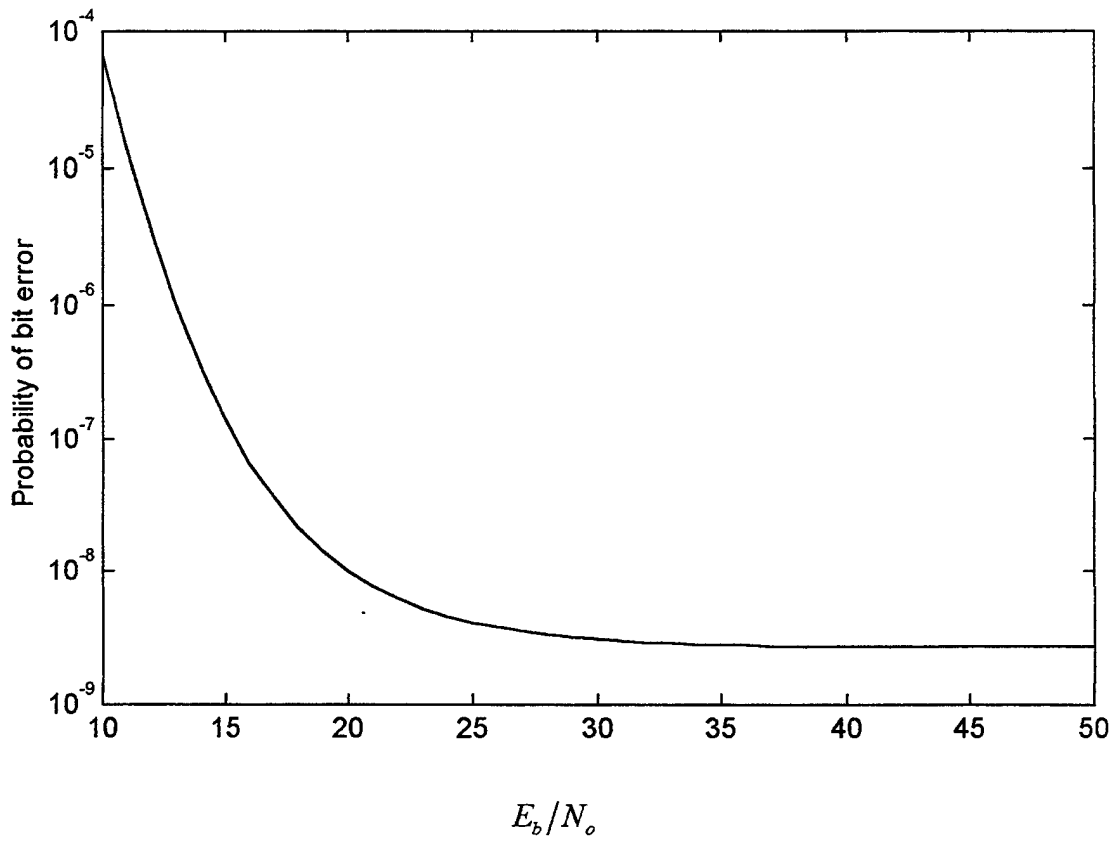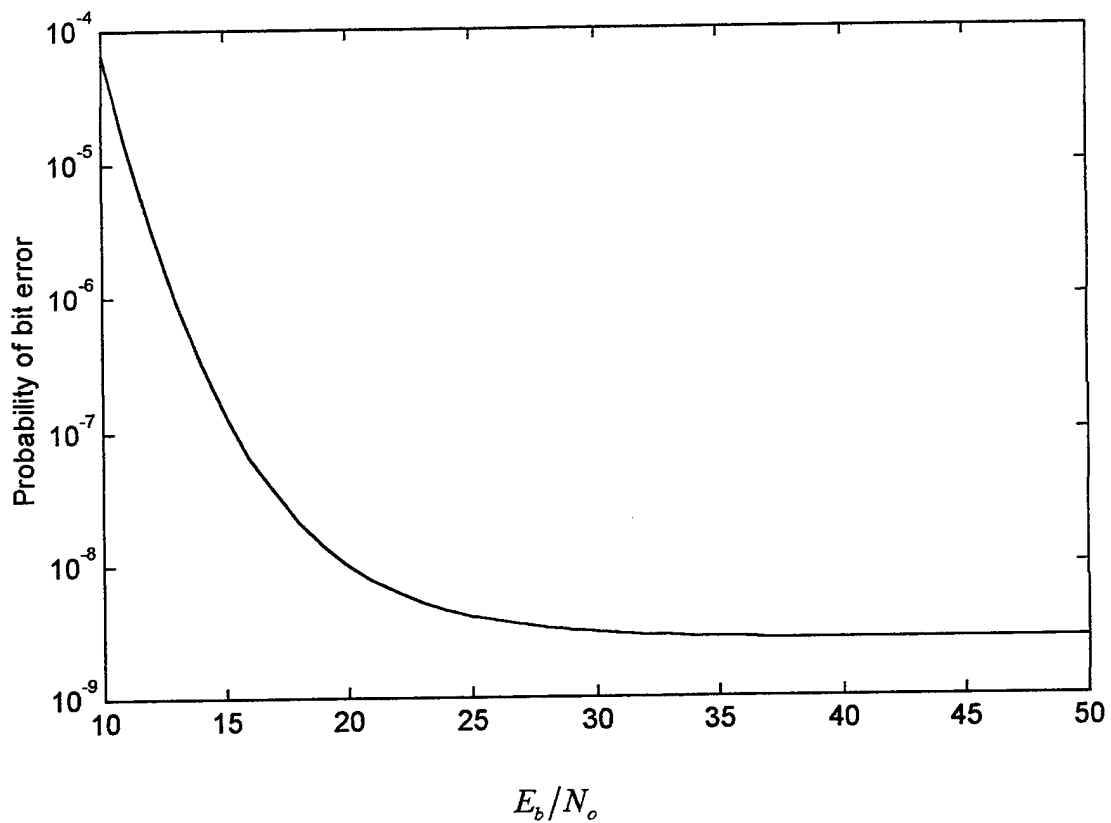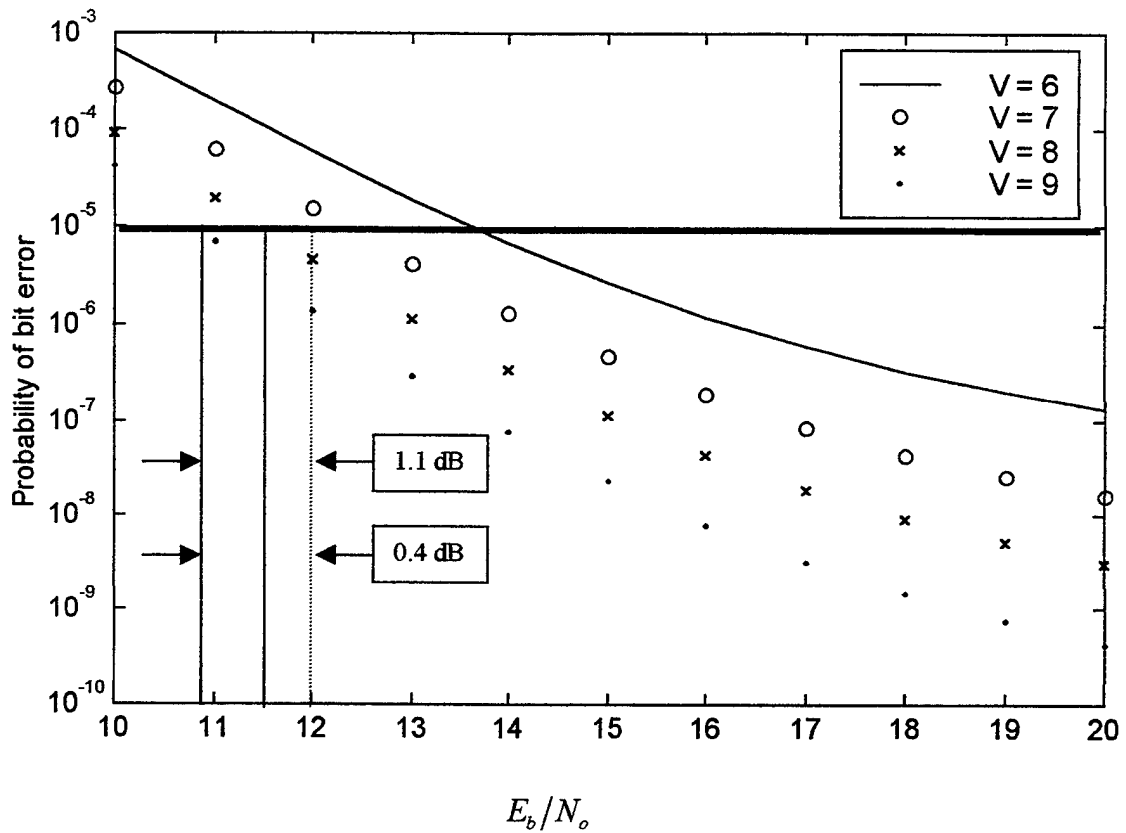
Figure 3.9. Reverse link performance using a Poisson distribution, a rate ½ convolutional code and with soft decision de⸱ ⸱ing. Simulation parameters are 23 users, constraint length varying from six to nine, processing gain of 32, and Poisson parameter of two.

For a signal-to-noise ratio of 12 dB, a processing gain of 16, and with the varying constraint lengths shown in Figure 3.8, the probability of bit error ranges from $10^{-3.2}$ to $10^{-4.5}$. The performance goal established in Chapter I is $P_b \leq 10^{-5}$ and is thus not met.

The performance calculation with the only change being a processing gain equal to 32 is repeated and the results illustrated in Figure 3.9. The resulting probability of error ranges from 10^{-4} to $10^{-5.9}$. Only the constraint length of eight and nine meet our performance goal. From Figure 3.9 we can observe that constraint lengths eight and nine have link margins of 0.4 and 1.1 dB, respectively. For PCS communications, where the frequencies are between 1500 MHz and 2000 MHz, the acceptable margin for suburban areas is 0 dB and for metropolitan centers is 3 dB [Ref. 3]. We will assume 2 dB. Our link margin does not meet this goal. Additionally, other forms of interference, such as co-channel interference, not included in our analysis may further reduce our actual performance.

The IS 95 standard for a narrowband CDMA reverse link uses a rate 1/3 convolutional code and a constraint length of nine [Ref. 3]. To make our PCS notebook as small as practical while maintaining a 2 dB margin and at most a $P_b \leq 10^{-5}$, we prefer to use a constraint length that is less than nine and a code rate that provides the highest date rate possible. To meet these requirements, we will investigate the use of concatenated coding.

F. UNCONDITIONAL UPPER BOUNDED PROBABILITY OF ERROR USING CONCATENATED CODING IN A RAYLEIGH CHANNEL

A concatenated code is a combination of two separate codes operating in series. The two codes are described as the outer and inner code. In our system we shall use a Reed-Solomon outer code with hard decision decoding and a convolutional inner code with soft decision decoding. The concatenated code rate (r_{cc}) is equal to the outer code rate (r_o) multiplied by the inner code rate (r_i). A block diagram of a concatenated coded communications system is illustrated in Figure 3.10 [Ref. 5].
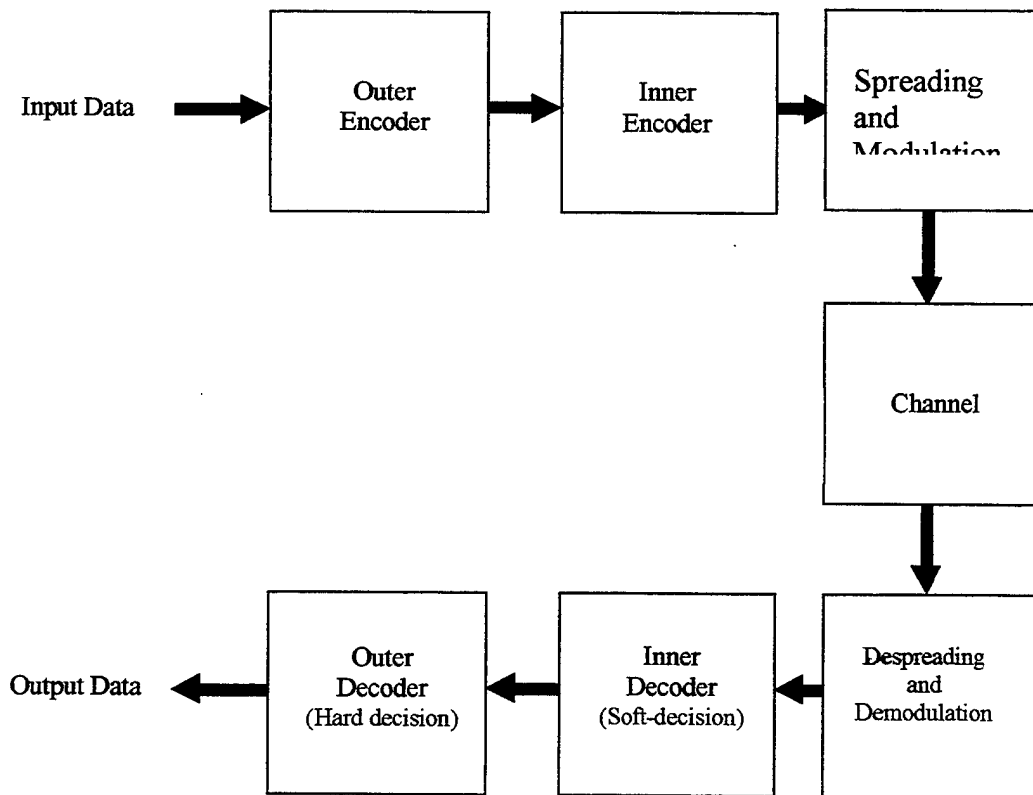
Figure 3.10. Block diagram of a concatenated coded communications system.

The source data stream is converted into k_o non-binary, m-bit symbols and encoded as n_o m-bit symbols by the Reed Solomon outer encoder. These n_o symbols are converted to a serial format for the inner binary convolutional encoder. After completing the convolutional encoding, the data is spread, modulated, and transmitted.

The received data stream is despread and demodulated prior to entering the inner decoder. The inner decoder, using soft decision Viterbi decoding, decodes the received data. The decoded bits are passed serially to the outer decoder. The probability of bit error at the inner decoder output is given by Equation 3.7. The outer decoder must place the serial data stream into m-bit symbols to allow hard decision Reed Solomon decoding. The reverse link uses binary modulation; therefore, the probability of coded symbol error at the input to the outer decoder is [Ref. 5]

$$p_s = 1 - (1 - P_b)^m \tag{3.10}$$

where $m = \log_2(n_o + 1)$ and P_b is equal to the probability of error of the inner convolutional code given by Equation 3.7. The output probability of bit error for Reed Solomon codes and hard decision decoding is [Ref. 5]:

$$P_{b_{cc}} \approx \frac{n_o + 1}{2 n_o^2} \sum_{i=t+1}^{n_o} \binom{n_o}{i} p_s^i (1 - p_s)^{n_o - i} \tag{3.11}$$

where n_o is the number of Reed Solomon coded bits, k_o is the number of Reed Solomon information data bits, and $t = \dfrac{n_o - k_o}{2}$.

G. UPPER BOUNDED PERFORMANCE OF DPSK USING CONCATENATED CODING OVER A RAYLEIGH CHANNEL

To compare performance, we plot plotted the probability of bit error for both concatenated and convolutional coding. The plot illustrated in Figure 3.11 is a comparison of a rate ½ convolutional code and a concatenated code with a rate of 0.44 using a 27/31 Reed Solomon outer code and a rate ½ convolutional inner code.

Figure 3.11. Reverse link performance using a Poisson distribution, a rate 27/62 concatenated code with an inner ½ convolutional code, an outer 27/31 Reed Solomon code, and soft decision decoding. Simulation parameters are K_{max} of 23, constraint length nine, processing gain of 32, and Poisson parameter of two.

The concatenated coding provides an additional coding gain of 1.7 dB with a total margin of 2.8 dB. To reduce receiver complexity, we reduce the constraint length to eight and plot the corresponding probability of bit. The results are depicted in Figure 3.12.

Figure 3.12. Reverse link performance using a Poisson distribution, a rate 27/62 concatenated code with an inner ½ convolutional code, an outer 27/31 Reed Solomon code, and soft decision decoding. Simulation parameters are K_{max} of 23, constraint length eight, processing gain of 32, and Poisson parameter of two.

The concatenated coding provides an additional coding gain of 2.5 dB with a total margin equaling 2.5 dB.

For constraint length seven, the corresponding probability of bit error for convolutional coding and concatenated coding is each depicted in Figure 3.13.
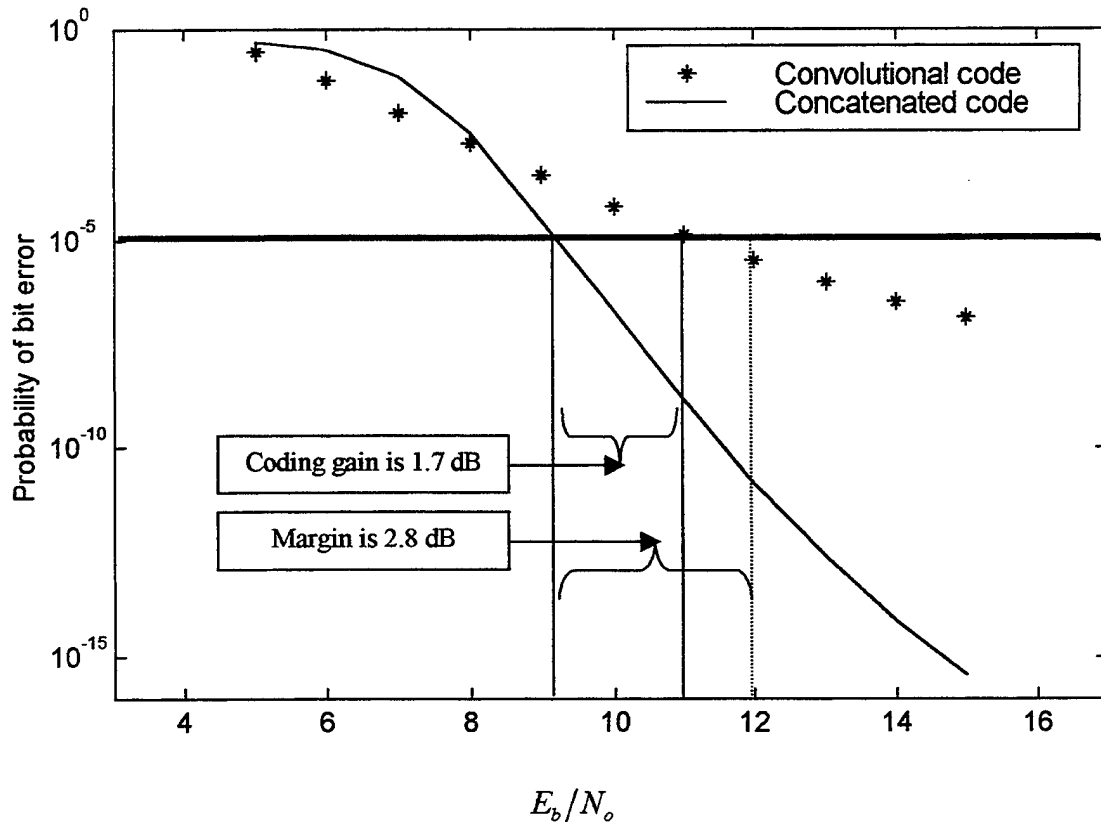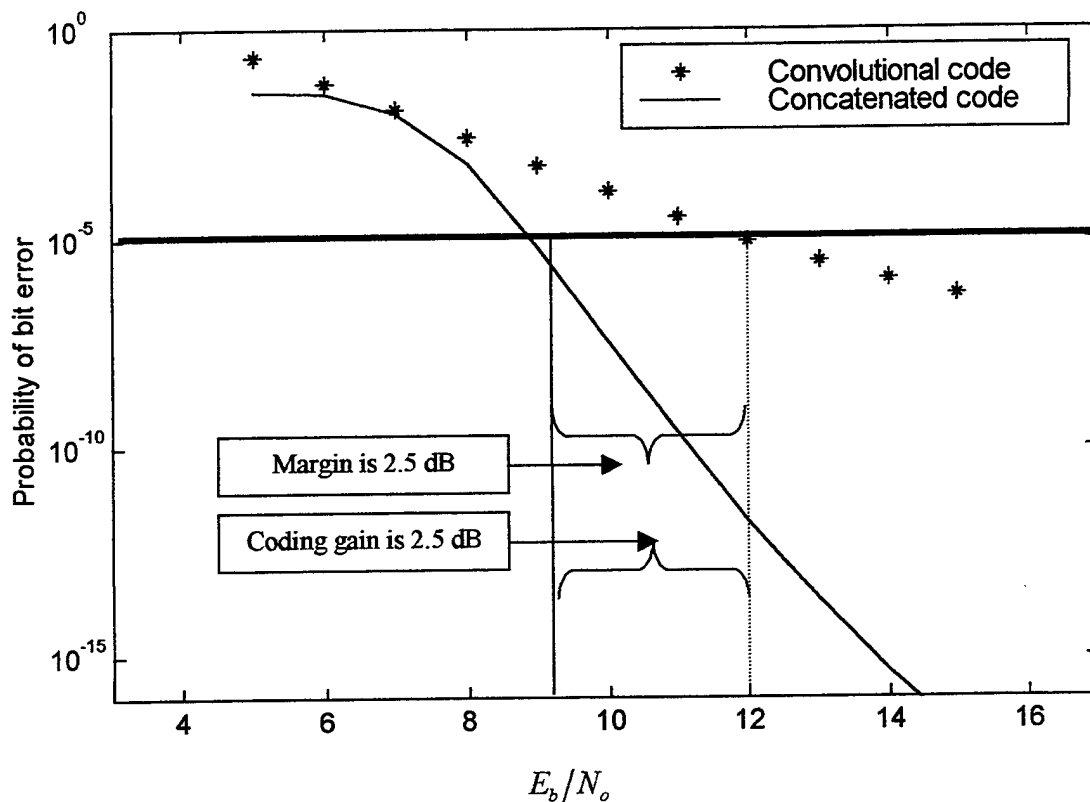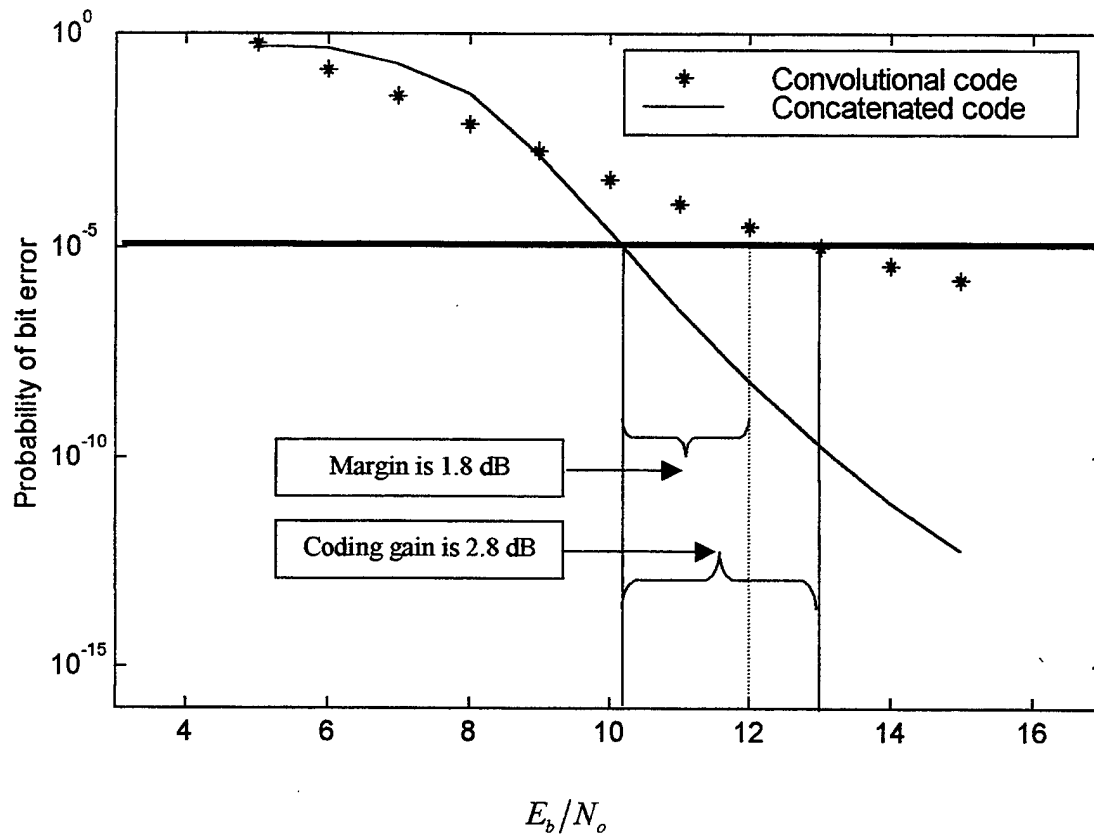
Figure 3.13. Reverse link performance using a Poisson distribution, a rate 27/62 concatenated code with an inner ½ convolutional code, an outer 27/31 Reed Solomon code, and soft decision decoding. Simulation parameters are K_{max} of 23, constraint length seven, processing gain of 32, and Poisson parameter of two.

In this case, concatenated coding provides a coding gain of 2.8 dB with a margin equaling 1.8 dB. The margin is below our goal of 2 dB. Therefore, constraint length 7 is not a consideration unless we are willing to consider reduced margin. Comparing Figure 3.9 with Figure 3.13, we see that the link margin of the concatenated system with constraint length 7 is superior to the convolutional coding alone with constraint length nine by 0.7 dB.

H.   REVERSE LINK CONCLUSIONS

To design a reverse link high data rate system, several challenges had to be resolved. Confining the modulated signal to within the FCC assigned bandwidth, the small physical size required by the mobile, the presence of multiuser interference, and fading significantly influenced our design decisions. A probability of bit error of 10^{-5} and a link margin of 2 dB were established as our performance criteria.

To remove the dependence on the number of users on SNR as shown in Equation 3.3, a distribution that represents the number of users on the system had to be selected. The Poisson distribution was selected over all other available distributions. The Poisson distribution allows us to assign the most likely number of users to be greater than one. Using the Poisson distribution and the law of total probability, we were able to derive the average probability of bit error for our system.

Increasing processing gain will increase signal-to-noise ratio and decrease probability of bit error, see Equations 3.3 and 3.7. Using convolutional coding, a constraint length of 6, 7, 8, and 9, and a processing gain of 16, we found that at a SNR of 12 dB a probability of bit error $\leq 10^{-5}$ was unachievable. Increasing processing gain to

32, we found that constraint lengths 8 and 9 yielded $P_{b_{CC}} < 10^{-5}$ while constraint length 6 and 7 gives unacceptable results.

Although the rate ½ convolutional code with constraint length 8 and 9 is able to achieve the probability of bit error goal, we see from Figure 3.9 that neither constraint length were able to provide a link margin greater ≥ 2 dB.

As illustrated in Figures 3.11 and 3.12, a multicarrier CDMA system using concatenated coding will produce a probability of bit error less than 10^{-5} and a link margin greater than 2 dB. The best performing system was found to be a concatenated code with a rate 27/31 Reed Solomon outer code and a rate ½ convolutional inner code constraint length 9 with a processing gain of 32, see Figure 3.11. This system achieved a probability of bit error at 12 dB SNR of 10^{-11} and a margin of 2.8 dB.

A concatenated code with the same outer code and a constraint length 8 rate ½ convolutional inner code produces a probability of bit error at 12 dB SNR of 10^{-12} and a margin of 2.5 dB, as illustrated in Figure 3.12. The smaller constraint length 8 code reduces transmitter complexity and allows smaller mobile PCS notebooks to be designed.

If we reduced the link margin required to 1 dB, from Figure 3.9 we see that the rate ½ convolutional code will provide a probability of bit error at 12 dB of $10^{-5.8}$ and a link margin of 1.1. This would avoid the complexity of the complexity of adding the concatenated code to our system while allowing the design of smaller PCS notebooks.

The concatenated code with a constraint length 8 convolutional inner code allows us to design small physical size PCS notebook while maintaining a link margin of 2 dB. The Reed Solomon code will require the data to be in $n_o m$ symbols for a total of 155 bits

per symbol. However, this is still below the number of bits per symbol transmitted by IS-95 or Global Systems Mobile (GSM) [Ref. 3]. For these reasons the concatenated code with a constraint length 8 rate ½ convolutional inner code and a processing gain of 32 was selected for the reverse link. In practice, the concatenated code can be implemented with an interleaver between the inner and outer codes to reduce the effect of burst errors.

IV.   FINDINGS AND CONCLUSIONS

This thesis has investigated the performance of a multicarrier broadband CDMA

cellular system. To ensure the system meets all FCC regulatory requirements, the system

analyzed complies with the PCS broadband standards outline in [Ref. 1]. The forward

and reverse links were designed to provide a probability of bit error $\leq 10^{-5}$ at a SNR of

12 dB, a link margin of 2 dB, and a maximum channel coherence bandwidth of 2.5 MHz

while considering the small physical size requirements of the mobile and the multiuser

environment.

A.   THE FORWARD LINK

To meet these performance goals, the forward link uses a pilot tone to coherently

receive a BPSK signal spread with a Walsh-Hadamard sequence. The Walsh-Hadamard

functions provide an orthogonal channelization for each base station-to-user signal. The

forward link pilot tone improves reception by providing a phase and timing reference.

These system features allow us to assume that intra-cell multiuser interference is much

smaller than the first tier co-channel interference. Proper cellular system design will

ensure the second tier co-channel interference is much smaller than the first tier.

Therefore, we assume the second tier co-channel interference is negligible.

Without forward error correction coding, our performance goals could not be met.

To minimize the decrease in data rate that occurs when using error correction, we

investigated the use of a rate ½ convolutional code. The rate ½ convolutional code with a

constraint length of nine when combined with a processing gain of 32 met our

performance goals.

In order to provide the user with a higher data rate and a physically smaller mobile, we investigated sectoring as a means of reducing both the processing gain and constraint length. As sectoring increases, link margin also increases, all other things being equal, assuming frequency re-use. Sectoring will result in a smaller PCS notebook and lower co-channel interference but will also result in either reduced processing gain or reduced overall system bit rate. Alternatively, for the same co-channel interference, capacity can be increased. Using 120-degree or 60-degree sectoring with frequency re-use, we met or surpassed our performance goals. A link margin of 5.9 dB was obtained using a 60-degree antenna system and a rate ½ convolutional code with a constraint length of nine for a processing gain of 16. We could further improve the system performance by using concatenated coding. However, the rate ½ convolutional codes already meet our design goals and can be implemented with less receiver complexity.

B.   THE REVERSE LINK

The reverse link must have the same performance as the forward link. To meet these performance goals, the reverse link uses a DPSK signal spread with a PN sequence. The reverse link is noncoherently received, and as a result, the probability of bit error is dependent on the number of users on the system. To remove this dependence, a distribution that is representative of the number of users on the system was selected. The Poisson distribution best modeled the expected system usage. Using the law of total probability and the Poisson distribution, we were able to derive the average probability of bit error for the reverse link. This analysis did not include co-channel interference.

Analysis with a processing gain of 16 or 32, and a constraint length of 6, 7, 8, and 9 revealed that a rate ½ convolutional code did not meet our performance requirements.

Using a concatenated code, we evaluated the system for the same range of processing gain and constraint lengths. The concatenated code with a constraint of eight or nine convolutional inner code and a Reed-Solomon outer code met our performance goals. The best performing system was found to be a concatenated code with a rate 27/31 Reed-Solomon outer code and a rate ½ convolutional inner code. The concatenated code with a constraint length eight convolutional code allows us to design a small physical size PCS notebook while maintaining our performance goals. Therefore, the concatenated code with constraint length eight and a processing gain of 32 was selected for the reverse link.

LIST OF REFERENCES

1. Longin I., *Broadband PCS Fact Sheet*, Wireless Telecommunications Bureau, Washington D.C., August 3, 1998.

2. Proakis J., *Digital Communications*, 3rd edition, McGraw Hill, New York, NY, 1995.

3. Rappaport T., *Wireless Communications*, Prentice Hall, Upper Saddle New Jersey, 1996.

4. Mehrotra A., *Cellular Radio Performance Engineering*, Artech House Publishers, Norwood, MA, 1994.

5. Robertson R.C., *"Communications Engineering Short Course,"* Dahlgren VA, November 20-22, 1996.

6. Mayer T., *"Co-Channel Interference Effects in a Wireless CDMA System,"* Master's Thesis, Naval Postgraduate School, Monterey, CA, August 1998.

7. Clark G. and Cain, J., *Error Correction Coding for Digital Communication*, Plenum Press, New York, NY, 1998.

8. Leon-Garcia, *Probability and Random Processes for Electrical Engineering*, 2nd edition, Addison Wesley Publishing Company, Reading, MA, 1994.

INITIAL DISTRIBUTION LIST

No. Copies

1. Defense Technical Information Center 2
    8725 John J. Kingman Rd., STE 0944
    Ft. Belvoir, VA 22060-6218

2. Dudley Knox Library 2
    Naval Postgraduate School
    411 Dyer Rd.
    Monterey, CA 93943-5101

3. Chairman, Code EC 1
    Department of Electrical and Computer Engineering
    Naval Postgraduate School
    Monterey, CA 93943-5121

4. Professor Tri Ha, Code EC/Ha 2
    Department of Electrical and Computer Engineering
    Naval Postgraduate School
    Monterey, CA 93943-5121

5. Professor R. C. Robertson, Code EC/Rc 2
    Department of Electrical and Computer Engineering
    Naval Postgraduate School
    Monterey, CA 93943-5121

6. LT Howard Pace Jr. 3
    Box 296 Waterworks Road
    London, KY 40741